Geochemistry Geophysics Geosystems G3
AN ELECTRONIC JOURNAL OF THE EARTH SCIENCES
Published by AGU and the Geochemical Society

Article
Volume 5, Number 10
21 October 2004
Q10006, doi:10.1029/2004GC000715
ISSN: 1525-2027

Composition and structure of the central Aleutian island arc from arc-parallel wide-angle seismic data

Donna J. Shillington
Department of Geology and Geophysics, University of Wyoming, Laramie, Wyoming 82071-3006, USA

Now at Southampton Oceanography Centre, University of Southampton, Southampton SO14 3ZH, UK (djshill@soc.soton.ac.uk)

Harm J. A. Van Avendonk
Institute for Geophysics, University of Texas at Austin, 4412 Spicewood Springs Road, Austin, Texas 78759-8500, USA

W. Steven Holbrook
Department of Geology and Geophysics, University of Wyoming, Laramie, Wyoming 82701-3006, USA

Peter B. Kelemen
Department of Geology and Geophysics, Woods Hole Oceanographic Institution, Woods Hole, Massachusetts 02543-1541, USA

Matthew J. Hornbach
Department of Geology and Geophysics, University of Wyoming, Laramie, Wyoming 82071-3006, USA

[1] New results from wide-angle seismic data collected parallel to the central Aleutian island arc require an intermediate to mafic composition for the middle crust and a mafic to ultramafic composition for the lower crust and yield lateral velocity variations that correspond to arc segmentation and trends in major element geochemistry. The 3-D ray tracing/2.5-D inversion of this sparse wide-angle data set, which incorporates independent phase interpretations and new constraints on shallow velocity structure, produces a faster and smoother result than a previously published velocity model. Middle-crustal velocities of 6.5–7.3 km/s over depths of ~10–20 km indicate an andesitic to basaltic composition. High lower-crustal velocities of 7.3–7.7 km/s over depths of ~20–35 km are interpreted as ultramafic-mafic cumulates and/or garnet granulites. The total crustal thickness is 35–37 km. This result indicates that the Aleutian island arc has higher velocities, and thus more mafic compositions, than average continental crust, implying that significant modifications would be required for this arc to be a suitable building block for continental crust. Lateral variations in average crustal velocity (below 10 km) roughly correspond to trends in major element geochemistry of primitive (Mg # > 0.6) lavas. The highest lower-crustal velocities (and presumably most mafic material) are detected in the center of an arc segment, between Unmak and Unalaska Islands, implying that arc segmentation exerts control over crustal composition.

Components: 14,537 words, 13 figures.

Keywords: continental crust; crustal geophysics; island arc; major element geochemistry.

Index Terms: 0903 Exploration Geophysics: Computational methods, potential fields; 1020 Geochemistry: Composition of the crust; 3025 Marine Geology and Geophysics: Marine seismics (0935).

Received 9 February 2004; **Revised** 23 July 2004; **Accepted** 23 August 2004; **Published** 21 October 2004.

Shillington, D. J., H. J. A. Van Avendonk, W. S. Holbrook, P. B. Kelemen, and M. J. Hornbach (2004), Composition and structure of the central Aleutian island arc from arc-parallel wide-angle seismic data, *Geochem. Geophys. Geosyst.*, *5*, Q10006, doi:10.1029/2004GC000715.

1. Introduction

[2] Island arcs are the surface manifestation of magmatism driven by subduction [e.g., *Coats*, 1952; *Marsh and Carmichael*, 1974; *Hamilton*, 1988]. The composition and structure of island arcs can distinguish between competing models for arc magmatic systems and for the creation of new continental crust. Compilations of crustal geochemical and geophysical data indicate that the bulk composition of the continental crust is equivalent to a high Mg # andesite (molar Mg/(Mg + Fe), or Mg # > 0.5,SiO_2 > 54 wt%) enriched in incompatible elements, with an average P wave velocity of ~6.45 km/s [*Smithson et al.*, 1981; *Braile et al.*, 1989; *Christensen and Mooney*, 1995; *Kelemen*, 1995; *Rudnick*, 1995; *Rudnick and Fountain*, 1995]. Lavas with this composition are observed only in arcs, giving rise to the hypothesis that the accretion of island arcs is a primary means of continental genesis and growth [e.g., *Taylor*, 1967; *McLennan and Taylor*, 1982]. The island arc models require either that the bulk composition and average velocity of island arcs are similar to that of continental crust or that island arcs are modified during or after accretion [e.g., *Smithson et al.*, 1981].

[3] While high Mg # andesites, enriched in rare earth elements, can be created in intraoceanic arcs [*Kelemen*, 1995; *Yogodzinski et al.*, 1995; *Hirose*, 1997; *Yogodzinski and Kelemen*, 1998; *Tatsumi*, 2001], the majority of extrusive material produced in this geologic setting is basaltic [*Myers*, 1988; *Plank and Langmuir*, 1988; *Rudnick*, 1995; *Kelemen et al.*, 2003a]. Consequently, some models call on the modification of a mafic arc to create continental crust. Proposals include reworking of intraoceanic island arcs by secondary melting [*Arndt and Goldstein*, 1989], magma mixing [*McBirney et al.*, 1987], delamination of lower-crustal cumulates [*Arndt and Goldstein*, 1989; *Kay and Kay*, 1993], or some combination thereof [*Arndt and Goldstein*, 1989; *Jull and Kelemen*, 2001; *Kelemen et al.*, 2003a] to reconcile apparent differences between the composition of island arcs and continental crust. Alternatively, although the majority of extrusive material produced in intraoceanic island arcs is basaltic [*Myers*, 1988; *Plank and Langmuir*, 1988; *Rudnick*, 1995], this does not require the middle and lower crust to be correspondingly mafic [*Kelemen*, 1995; *Kelemen et al.*, 2003c]. Rising andesitic magmas, unlike their mafic counterparts, might crystallize in the lower and/or middle crust due to their relatively high viscosity, and thus be selectively preserved [*Kay et al.*, 1990; *Kelemen*, 1995; *Kelemen et al.*, 2003c]. The presence or absence of andesitic material in the middle and/or lower crust bears on the question of how arcs contribute to the amalgamation of continental crust and provides insight into the magmatic processes in intraoceanic island arcs.

[4] Intraoceanic island arcs offer the opportunity to study the composition of arc middle and lower crust in a place where the effects of preexisting material (e.g., continental crust) are minimal. The Aleutian island arc provides an ideal natural laboratory for the investigation of intraoceanic island arcs. Extensive geochemical data on extrusive rocks and xenoliths [*Class et al.*, 2000; *Myers and McElfresh*, 2001; *Kelemen et al.*, 2003c], earthquake studies [*Ekström and Engdahl*, 1989; *Engdahl et al.*, 1989; *Abers*, 1994] and GPS studies [*Mann et al.*, 2002; *Mann and Freymuller*, 2003] are also available from the central Aleutian island arc, in addition to multichannel seismic (MCS) reflection and wide-angle reflection/refraction data [*McGeary and Group*, 1996; *Fliedner and Klemperer*, 1999; *Holbrook et al.*, 1999; *Fliedner and Klemperer*, 2000; *Lizarralde et al.*, 2002] (Figure 1). In this paper, we present a new velocity model of an 800-km-long wide-angle seismic reflection/refraction line (line A2), which parallels the central Aleutian island arc, extending from Atka Island to Unimak Island, and compare crustal velocities to geochemistry along the arc. *Fliedner and Klemperer* [1999, 2000] published the first interpretations of this data set. Our model incorporates independent phase interpretations and new data on shallow levels of the arc not included in previously published models; reflections and refractions from MCS shot gathers and seafloor bathymetry are included to constrain shallow heterogeneity along the shot line. A 3-D ray tracing/2.5-D inversion approach [*Van Avendonk et al.*, 2004] was used to produce a robust seismic velocity result. We also compare line A2 velocity structure with along-arc geochemistry, compiled by *Kelemen et al.* [2003c], and with

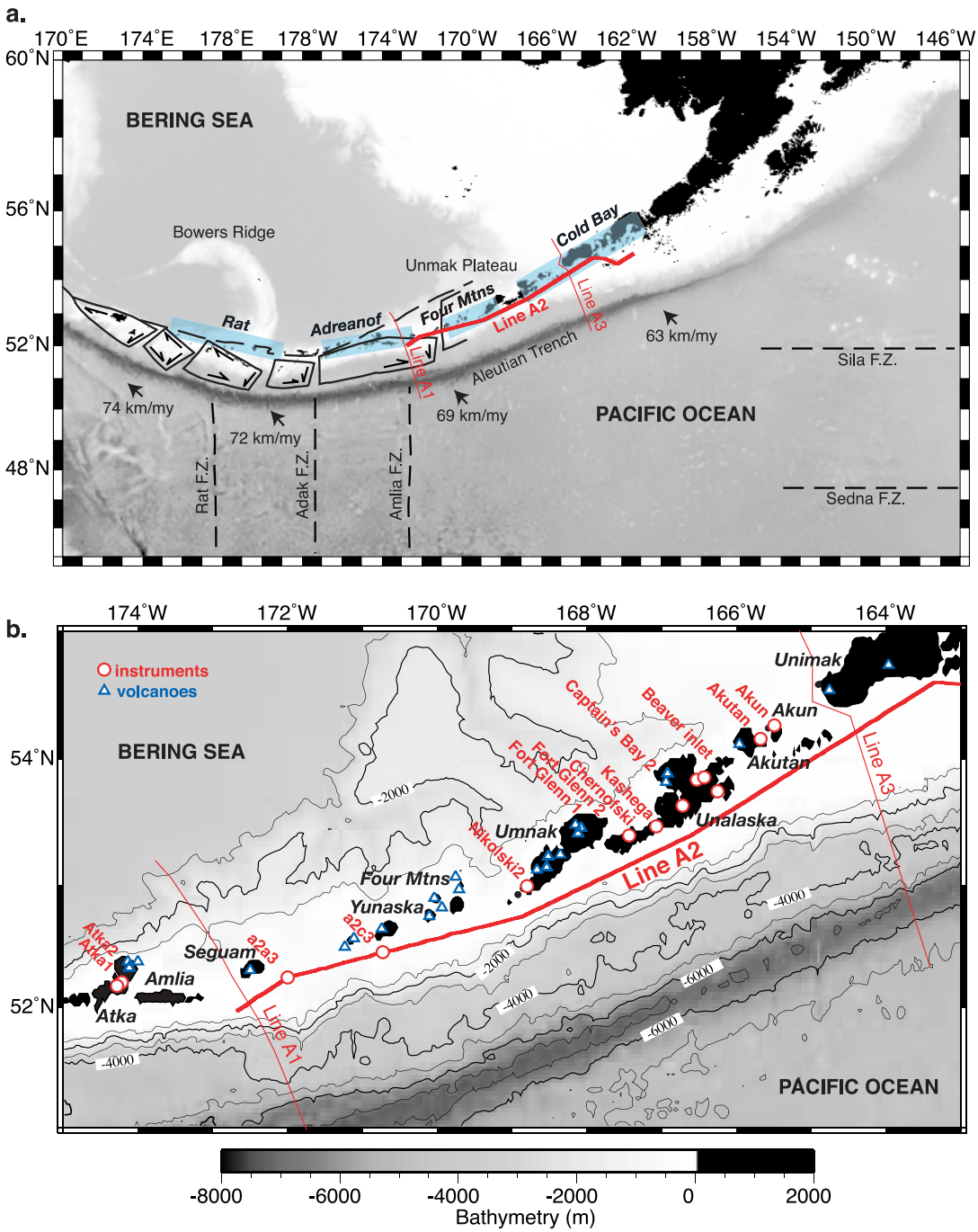

Figure 1. Bathymetric maps showing the location of the 1994 Aleutians Experiment. The ship track of the R/V *Maurice Ewing* along line A2, which extends along the arc from Atka Island to Unimak Pass, is indicated with a thick red line. Bathymetry is taken from GEBCO [*Intergovernmental Oceanographic Commission and International Hydrographic Organization*, 2003]. Thin red lines indicate the locations of cross-arc lines A1 and A3 [*Holbrook et al.*, 1999; *Lizarralde et al.*, 2002]. (a) Map showing tectonic and geographic framework of 1994 Aleutians experiment. Black lines and arrows indicate the arc segmentation and rotation described by *Geist et al.* [1988] based on structural studies. Blue boxes and text show arc segmentation suggested by *Kay et al.* [1982] based on geochemistry. Arc segmentation has been correlated with systematic changes in geochemistry and temperature along the central Aleutian arc [e.g., *Kay et al.*, 1982; *Singer and Myers*, 1990]. The locations of fracture zones and other large bathymetric features are also labeled with black lines and text. (b) Map showing the region immediately surrounding line A2. Portable land seismometers and ocean bottom seismometers, which are plotted as red circles with text, recorded air gun shots fired by the R/V *Maurice Ewing*. The locations of select volcanoes are indicated with blue triangles. The ship track along line A2 is indicated with a thick red line.

arc segmentation [*Kay et al.*, 1982; *Geist et al.*, 1988]. Our final velocity model contains higher velocities than the model of *Fliedner and Klemperer* [1999], a distinct three-layer structure, middle-crustal velocities indicative of intermediate and mafic plutonism, and lower-crustal velocities indicative of mafic and ultramafic cumulates. Our result demonstrates that the Aleutian island arc is significantly more mafic that continental crust. The highest lower-crustal velocities occur in the center of an arc segment, implying that segmentation of the upper plate exerts control over crustal composition.

2. Geologic Background

[5] The Aleutian island arc-trench system extends 3000 km from the Kamchatcka Peninsula to the Gulf of Alaska [*Fournelle et al.*, 1994; *Plafker et al.*, 1994; *Vallier et al.*, 1994]. The Pacific Plate lithosphere subducts beneath oceanic material west of Unimak Pass, and to the east of Unimak, the Pacific plate is subducting beneath Early Permian and Mesozoic accreted terranes and volcanics [*Fournelle et al.*, 1994]. The majority of oceanic crust west of Unimak Pass is probably derived from the relic Kula plate, though the origin of Bering Sea crust is poorly constrained and likely includes other terranes [*Marlow and Cooper*, 1983; *Cooper et al.*, 1992]. At 59 Ma, both the Kula plate and the Pacific Plate were subducting in the Aleutian trench, and these two plates were separated by a transform fault. At 56 Ma, subduction jumped south, stranding a small piece of the Kula plate ("Aleutia") on the North American plate [*Marlow and Cooper*, 1983]. At 40 Ma, the Kula plate subducted entirely, and the direction of convergence shifted from north to north-northwest.

[6] Despite the complexity added by the entrapment of the Kula plate and changes in the rate and direction of convergence, the Aleutian island arc still remains one of the best examples of a classic intraoceanic arc, free of some of the complications encountered in the investigation of other arcs. Subduction in the central Aleutians, the focus of this study, is currently nearly perpendicular to the trench (Figure 1a), with a convergence rate of 60–75 mm/yr, although subduction becomes more oblique westward [*DeMets and Dixon*, 1999]. The location of volcanism has only varied slightly over the last 20 m.y. [*Fournelle et al.*, 1994]. The central Aleutians have experienced comparatively little intra-arc extension or compression, although major element compositions and Sr isotopic characteristics have been interpreted as suggesting that some extension occurs above the subduction of the Amlia Fracture Zone (FZ), Adak FZ and Rat FZ [*Singer and Myers*, 1990; *Kay and Kay*, 1994]. Additionally, calculations based on earthquake slip vectors yield an arc-parallel extensional strain rate of $\sim 3.0 \times 10^{-8}$ yr^{-1} [*McCaffrey*, 1996].

[7] The locations of fracture zones in the subducting plate, together with the locations of the Bowers Ridge, transitions in upper plate composition (e.g., from oceanic to continental) and earthquake aftershock zones, have provided the basis for dividing the upper plate into four discrete "segments": Rat, Adreanof, Four Mountains, and Cold Bay [*Kay et al.*, 1982; *Kay and Kay*, 1994] (labeled with blue boxes and text, Figure 1a). The size and composition of volcanoes show an approximate variation from the edges of these segments to their centers. Large tholeiitic volcanoes tend to lie on segment ends and small, relatively felsic, calc-alkaline volcanoes tend to occur in segment centers [*Kay et al.*, 1982; *Kay and Kay*, 1994]. More recent studies based on stress homogeneity and earthquake distribution suggest further segmentation of the overriding plate, which may not correspond exactly to fracture zones or other features on the subducting plate [*Geist et al.*, 1988; *Nishenko and Jacob*, 1990; *Lu and Wyss*, 1996]. Structural investigations of arc segmentation indicate that blocks are rotating counterclockwise due to changes in Pacific Plate subduction direction and coupling between the Pacific and North American plates [*Geist et al.*, 1988] (Figure 1a), particularly west of Adak Island. Line A2, the focus of this study, lies primarily within the Four Mountains and Cold Bay blocks, except the western portion of the line, which lies west of the subduction of the Amlia FZ in the Adreanof block (Figure 1a). The specific geometry of upper plate segmentation, and its implications for changes in the stress regime within the Aleutian island arc, is important because it might exert control on the composition and volume of magmatic activity along the arc and on along-arc changes in the geothermal gradient [*Kay et al.*, 1982; *Singer and Myers*, 1990; *Singer et al.*, 1992; *Kay and Kay*, 1994].

[8] Four major element suites are represented in extrusive rocks erupted on the Aleutian Islands: (1) high-Mg tholeiitic basalts [*Myers*, 1988; *Kay and Kay*, 1994], (2) high-Mg calc-alkaline basalts and andesites [*Kay and Kay*, 1994], (3) low-Mg, high-Al basalts [*Baker and Eggler*, 1983; *Myers*

et al., 1985; *Myers*, 1988; *Brophy*, 1989], (4) enriched, high-Mg # andesites [*Kay*, 1978; *Kelemen*, 1995; *Yogodzinski et al.*, 1995; *Kelemen et al.*, 2003c]. Of these, low-Mg, high-Al and high-Mg basalts are the most abundant in the central part of the Aleutian island arc. Explanations for the occurrence of these diverse geochemical signatures in one island arc include variability in the source of parental magmas [*Miller et al.*, 1992], the effects of lithospheric structure [*Kay et al.*, 1982; *Singer and Myers*, 1990; *Singer et al.*, 1992; *Kay and Kay*, 1994], and changes in the parental magma during ascent due to fractionation, contamination or crystallization [*Myers*, 1988; *Kay and Kay*, 1994]. Lateral changes in middle and lower-crustal velocity (which will be controlled primarily by major element geochemistry and temperature) can illuminate some of the causes for larger geochemical diversity in the Aleutians. If models calling for the control of extrusive geochemistry by arc segmentation are correct, corresponding variations in crustal velocity should be observable in wide-angle velocity models.

3. Data Set and This Experiment

[9] The wide-angle reflection/refraction data used in this study are part of a larger seismic data set that includes both MCS reflection and wide-angle reflection/refraction data collected along three transects, two perpendicular to the Aleutian island arc (lines A1 and A3) [*Holbrook et al.*, 1999; *Lizarralde et al.*, 2002], and one along the arc (line A2) [*Fliedner and Klemperer*, 1999, 2000], as well as data collected in the Bering Sea [*Lizarralde et al.*, 2002] (Figure 1a). Line A2, the subject of this paper, is an ~800-km-long transect parallel to the central Aleutian island arc (Figure 1b). MCS reflection data were acquired on the 4-km streamer of the R/V *Maurice Ewing* at a sampling interval of 4 ms. Wide-angle data were acquired by portable land seismometers positioned on islands between Atka and Unimak and two ocean bottom seismometers positioned between Atka and Umnak. These instruments recorded shots from the R/V *Maurice Ewing*, which traveled south of the Aleutian Islands. Several instruments recorded only shots fired along lines A1 and A3; data from these instruments were not included in this study because the majority of these ray paths do not lie parallel to the arc, unlike other instruments along line A2. Shot spacing ranged from 34 to 61 m, and the sampling interval on most instruments was 10 ms. The ray paths resulting from the source-receiver geometry span a 3-D volume along line A2. Land instrument positions lie between 20 and 60 km north of the shot line, which itself parallels the arcuate island chain. This geometry presented two challenges: (1) shallow structure along the shot line and around receivers was not constrained by data recorded on OBS or portable seismometers; (2) ray paths from the shot line to the receivers travel over a large 3-D region (9.6×10^5 km^3), but are too sparse to constrain full 3-D structure.

[10] While 3-D in nature, this along-arc transect presents a unique opportunity to understand arc properties. Cross-arc lines measure arc properties across one section of the arc, while arc-parallel lines allow for the detection of changes in arc properties along the arc and comparisons with extrusive geochemistry. To deal with the sparse, 3-D nature of this data set, we used a 3-D ray tracing/2.5-D inversion scheme that accounts for shallow 3-D structure (on the shot line and at the receivers) but constrains the middle and lower crust to remain constant perpendicular to the arc [*Van Avendonk et al.*, 2004]. Although rays are traced in a 3-D model, ray coverage is too sparse to constrain the velocity characteristics on a 3-D rectangular grid. As a result, the number of model parameters must be decreased, and one logical manner in which to limit the degrees of freedom in inversion is to assume that the velocity structure is constant in the cross-arc direction [*Van Avendonk et al.*, 2004]. Our modeling approach is discussed in greater detail in another section of this paper and is fully described by *Van Avendonk et al.* [2004].

4. Data Processing

[11] Prior to phase correlation and modeling, wide-angle data underwent several premodeling processing steps, including band-pass filtering, predictive deconvolution and recalculation of shot-receiver offsets. Zero-phase, 8-pole, Butterworth band-pass filters limited data frequencies to 4–20 Hz and were carried out in the frequency domain. Least squares, predictive deconvolution was applied using 1% prewhitening, a filter length of 0.5 and a prediction distance of 0.05 s to remove "ringy" appearance of some phases. An offset-dependent gain was also applied for data plotting.

[12] Similar processing was applied to MCS shot gathers employed to create a shallow velocity model along the shot line. Frequency domain, minimum phase band-pass filters limited data frequencies to 4–80 Hz. Predictive deconvolution

with 1% prewhitening, filter length of 0.4 and a prediction distance of 0.2 s were also applied.

5. Shallow Structure Constraints From MCS Shot Gathers

[13] The velocity model previously constructed from this data set does not incorporate information on the shallow structure along the shot line, including seafloor topography [*Fliedner and Klemperer*, 1999, 2000]. The minimum offset recorded on most land stations was 20 km, so that no information on the shallow features (less than ~6–7 km depth) along line A2 is present in the wide-angle receiver gathers. The shallow velocity structure along strike is important to this study because travel time delays caused by shallow heterogeneities, such as sedimentary basins, can be propagated into deeper regions of the velocity model if ignored. Shallow structures vary significantly along line A2; *Lizarralde et al.* [2002] describe five sedimentary and upper-crustal layers in their velocity model of line A3, which crosses the arc at Unimak Pass. Four of these laterally varying upper-crustal layers are constrained by turning waves with offsets less than 25 km. Given that the minimum offsets in the wide-angle data recorded on land stations studied are usually between 20 and 30 km, little information on this complicated shallow structure is contained by the wide-angle data set. Because interpretations concerning the composition of the deeper crust are sensitive even to small fluctuations in velocity (0.1–0.5 km/s), these shallow structures need to be incorporated in a complete velocity model.

[14] To account for some of the shallow variability along the shot line on line A2, refractions and reflections representing sedimentary and basement structure were picked on the first 2 s of shot gathers recorded on the R/V *Maurice Ewing*'s 160-channel, 4-km streamer, and seafloor depth was taken from multibeam bathymetry acquired along line A2 by the R/V *Maurice Ewing*. MCS shot gathers along line A2 commonly recorded refractions from the sedimentary cover and uppermost basement and reflections from the top of crystalline basement (Figure 2). Sedimentary velocities varied vertically between 1.9 and 4.0 km/s. Uppermost crustal velocities varied between 4.15 and 4.45 km/s. Figure 2a shows shot gather 22760; note the basement reflection at 1.25 s and an offset of 2200 m and the basement refraction at 1.7 s and an offset of 3500 m.

[15] Over 1000 MCS shot gathers (every 20th gather along line A2, roughly spaced at 1 km) were used to build a 2-D model of the shallow structure along the shot line on line A2 in Rayinvr [*Zelt and Smith*, 1992]. Reflections from the seafloor and top of basement and refractions through the sediments and uppermost crust were interpreted on each shot gather where present. Around 14,650 picks with assigned errors of 0.1 s were included in the analysis. We found a seismic velocity model for the shallow basement and overlying sediments by fitting MCS shot gathers with a data misfit, χ^2, of 0.76 and a RMS travel time residual of 0.086 (Figure 3). This model was incorporated in the crustal model for accurate representation of the shallow structure beneath the shot line, and the sediments and basement depth were left fixed during inversion of the wide-angle data [*Van Avendonk et al.*, 2004]. Velocity information is unavailable on a section of upper crust below the reach of turning waves recorded on the MCS streamer and above the reach of turning waves recorded on land seismometers; in these sections, upper crustal velocities in our initial velocity model were taken from other velocity models in this region that contain information on shallow crust [*Abers*, 1994; *Holbrook et al.*, 1999; *Lizarralde et al.*, 2002]. The inclusion of information on the shallow structure along line A2 accounted for a significant amount of the small-scale variability observed in crustal arrivals in the wide-angle records. The magnitude of basement topography was as great as 1 km (e.g., near model km 220 and 700). Given that sediment velocities were usually ~2 km/s and uppermost crustal velocities ~4–5 km/s, neglecting variations in shallow structure could impart a maximum error of 250 ms. More common variations in topography of 0.25–0.5 km could introduce delays of ~100 ms.

[16] Shallow velocity structure beneath the individual receivers was accounted for by applying constant travel time shifts. A shift of 0.4 s accounted for the shallow structure of the volcanic islands where eleven land seismometers were deployed; upper crustal velocity structure is likely different beneath islands compared to other parts of the arc [*Van Avendonk et al.*, 2004]. No travel time shift was applied to receiver gathers recorded by ocean bottom seismometers.

6. Phase Correlation

[17] Phase correlation of crustal arrivals on instruments along line A2 was accomplished by com-

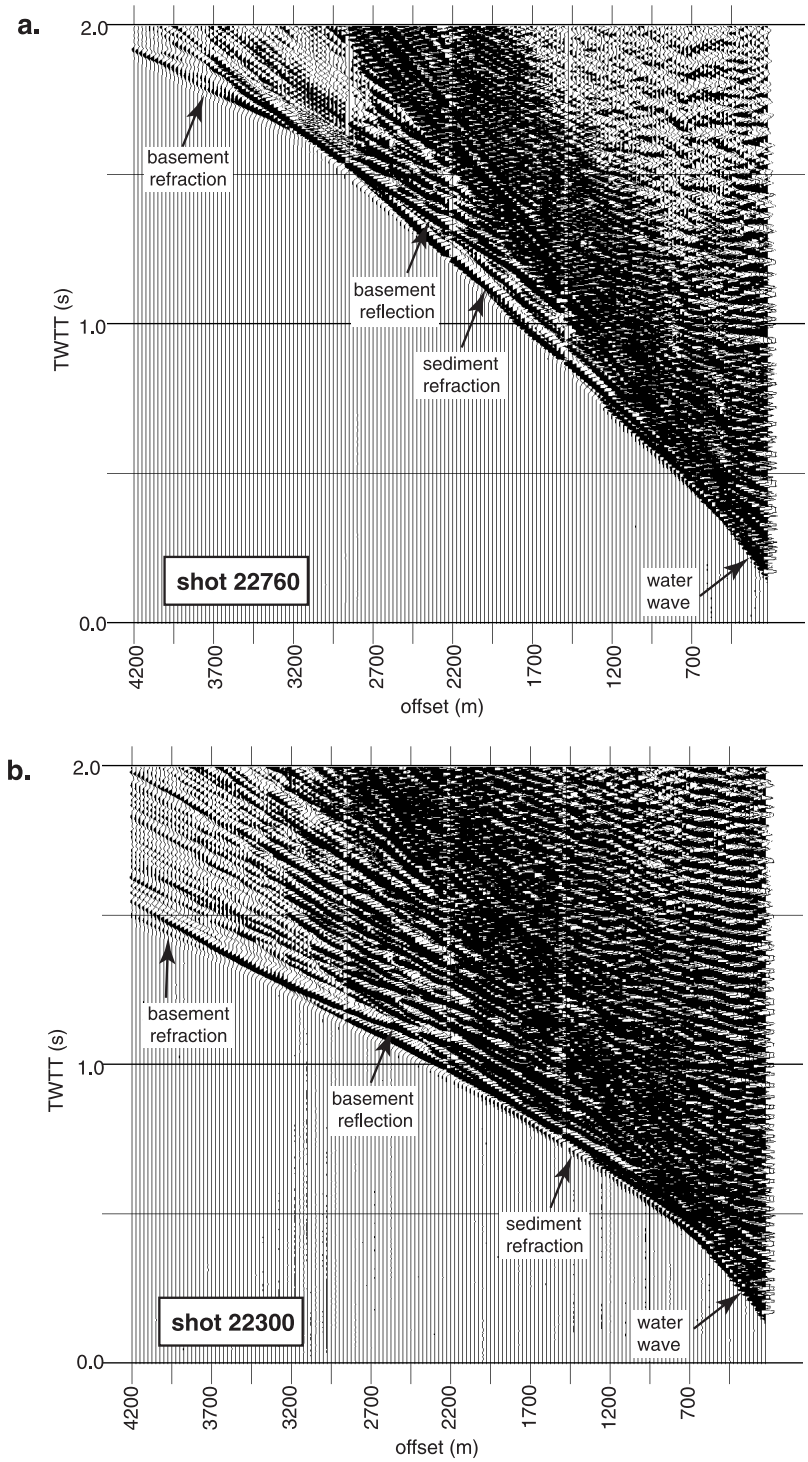

Figure 2. Examples of shot gathers recorded on the 180-channel streamer of the R/V *Maurice Ewing*. Each of these shot gathers shows direct arrivals, refractions through sedimentary layers and basement, and reflections off the top of basement; each of these phases is indicated with an arrow and text. Picks from the shot gathers were used to constrain shallow structure along line A2, shown in Figure 3. (a) Shot 22760; (b) shot 22300.

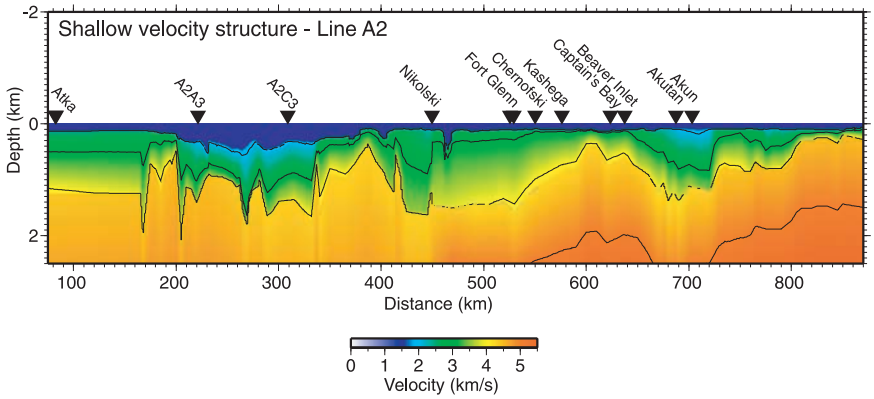

Figure 3. Shallow velocity structure (upper 2 km) along line A2 derived from 2-D ray tracing and inversion of picks from MCS shot gathers (e.g., Figure 2). The locations of portable land seismometers are indicated with inverted black triangles and text.

parison of adjacent receiver gathers and repeated checks for phase reciprocity. Because of the 3-D nature of the experiment, "reversed" arrivals recorded by adjacent instruments do not follow the exact same path through the arc, though the paths are very similar (note plan view of ray paths, Figure 4). Although the lack of true reversed ray paths limited reciprocity checks to ~0.2 s in some cases, the records show a consistent pattern of phases, shown in Figure 5. Greater detail on arrivals that characterize each layer is given in the following sections. Figures 6a–6m shows records of all instruments, with and without phase interpretations. Reflections and refractions in the upper and middle crust have assigned picking errors of 0.1 s, while deeper arrivals have assigned errors of 0.15–0.2 s.

[18] Reflections and refractions identified in wide-angle data delineate three distinct crustal layers and the uppermost mantle in some places. While apparent velocity varies within each crustal layer,

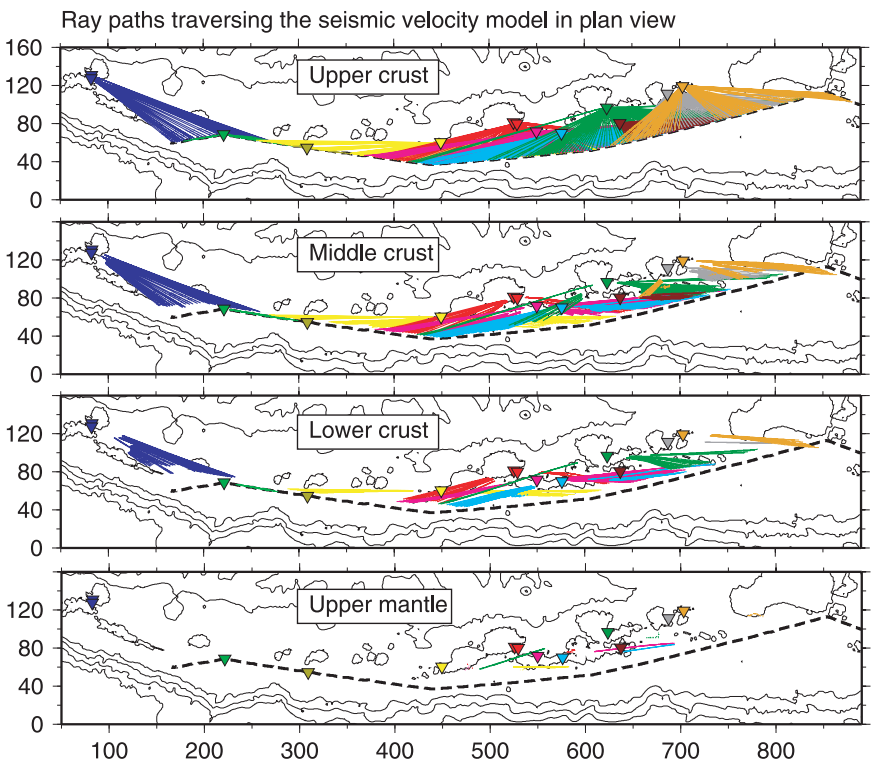

Figure 4. Ray paths traversing the seismic velocity model in plan view. Note that the majority of the paths of the rays lie parallel to the arc within the arc platform, 20 km trenchward of the active volcanic line.

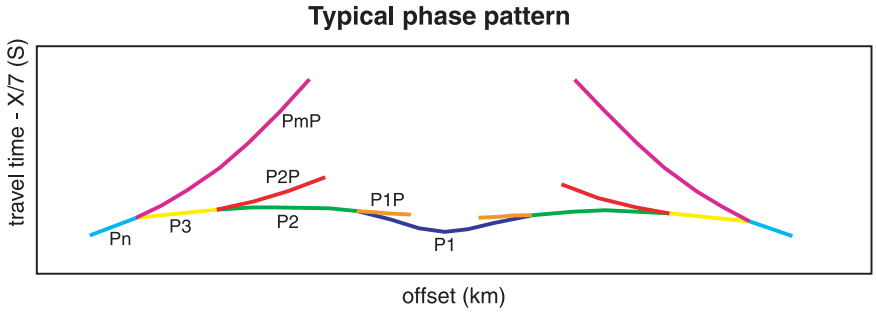

Figure 5. Generalized phase pattern. These phases are consistently observed on instruments along the entire 800-km span of line A2. P1 samples the upper crust (blue), P2 samples the middle crust (green), P3 samples the lower crust (yellow), and Pn samples the upper mantle (turquoise). Reflections (P1P (orange), P2P (red), and PmP (purple)) attend each of these refracted phases, suggesting discrete vertical velocity layering in the central Aleutian island arc along line A2.

particularly in the shallowest crustal layer, the three-layer interpretation of crustal phases is required because refracted waves bound by reflections and showing distinct apparent velocities are observed. Figure 6e shows a record from Nikolski2, which lies approximately in the center of line A2 and shows three-layer structure very clearly. Note the clear triplications between refractions P1 and P2 and between P2 and P3. A three-layer structure within the Aleutian island arc is also observed in wide-angle data collected on cross-arc lines A1 and A3 [*Holbrook et al.*, 1999; *Lizarralde et al.*, 2002].

7. Wide-Angle Modeling Procedure

[19] *Fliedner and Klemperer* [1999, 2000] used a 3-D finite difference ray tracing and inversion scheme to obtain a velocity model along line A2 [*Hole*, 1992; *Hole and Zelt*, 1995]. Because of the sparse nature of this data set, we chose to use a 3-D ray tracing/2.5-D inversion code [*Van Avendonk et al.*, 2004], an extension of the code used by *Van Avendonk et al.* [2001], to improve the constraints on inversion. The derivation and parameterization of this modeling strategy are described completely by *Van Avendonk et al.* [2004]. Ray tracing is conducted in three dimensions, but the inversion does not allow velocities to vary perpendicular to the arc. The splines used in tomographic inversion represent the seismic velocity averaged across the arc platform [*Van Avendonk et al.*, 2004]. Thus three-dimensional (3-D) structure in the shallow portion of the model is accommodated by incorporating a shallow velocity model along the shot line and by static time shifts at the land receivers, but the deeper structure is assumed to be two-dimensional [*Zelt and Zelt*, 1998]. Given that most ray paths recorded in this experiment are broadly arc parallel, with the majority of their paths lying approximately 20 km trenchward of active arc within the arc platform, this assumption of cross-arc homogeneity seems to be reasonable (Figure 4). Previous velocity models that cross the Aleutian arc between Seguam and Amlia Islands and at Unimak Pass indicate cross-arc homogeneity within the arc platform, which also justify this approach, although lower-crustal velocities increase abruptly in the forearc [*Holbrook et al.*, 1999; *Lizarralde et al.*, 2002].

[20] The starting model used for inversion must reproduce the observed pattern of arrivals; the detection of refractions through the middle and lower crust, particularly, places strong constraints on this model. The velocity structure used as a starting model is similar to the arc velocity structure obtained from inversion of P and S wave arrivals from local earthquakes [*Abers*, 1994].

8. Model Description

[21] Our final velocity model contains three discrete velocity layers, with velocities of 6.5–7.3 km/s in the middle crust for a depth range of ~10 to 20 km, 7.3–7.7 km/s in the lower crust for a depth range of ~20 to 35 km, and a total crustal thickness of 35–37 km. Figures 7a–7m show picks and model predictions for each instrument. The final velocity model has a normalized χ^2 of 1.46 and a RMS misfit of 0.133 s, and it is shown in Figure 8. *Van Avendonk et al.* [2004] discuss the error statistics for individual layers, the uncertainties associated with crustal velocities and thicknesses, and the ability of this data set and method to resolve small-scale structure. Resolution analysis suggests that the primary features (>50 km

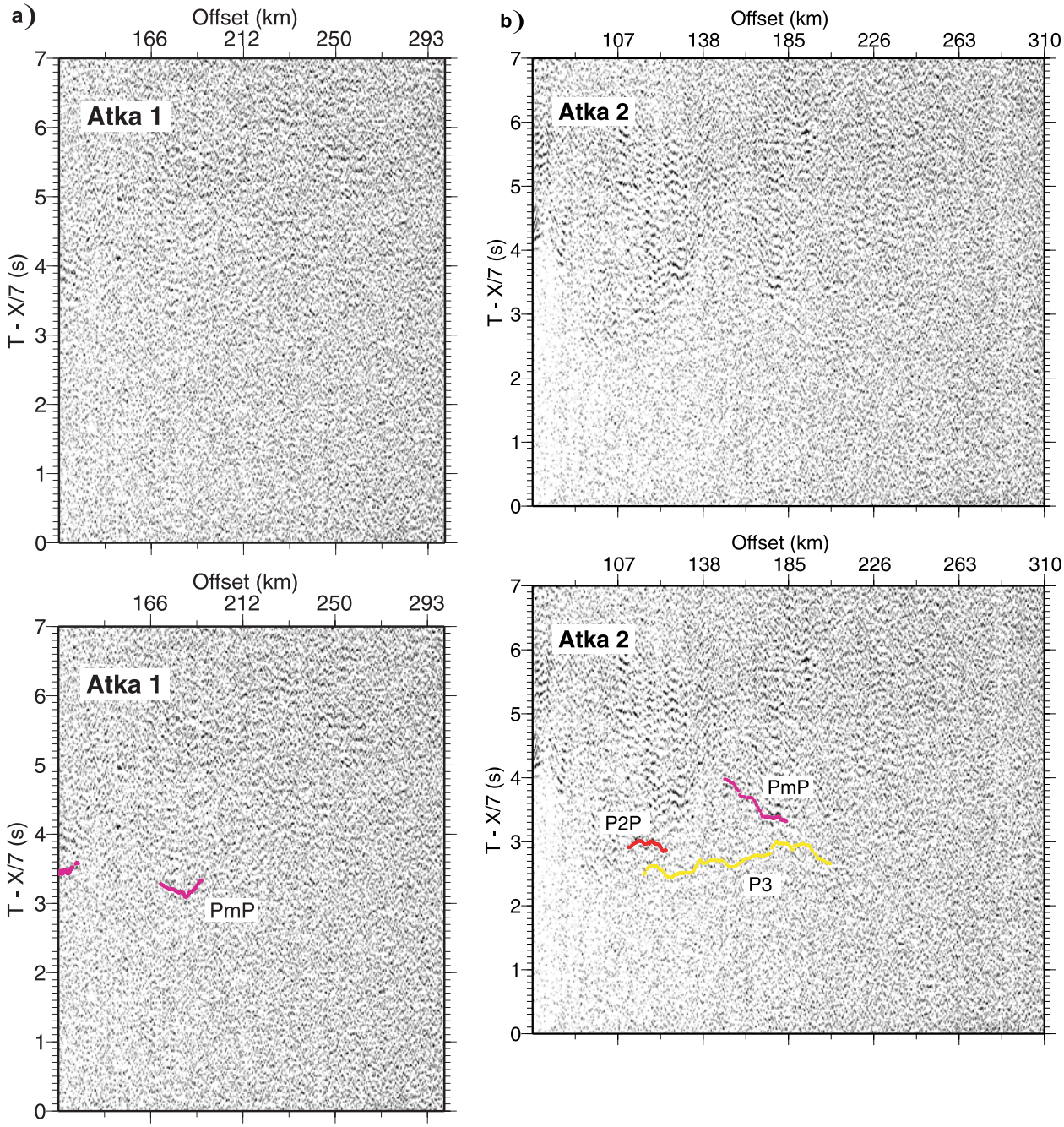

Figure 6. Plots of receiver gathers used in creating velocity model, with and without phase interpretations. Phase interpretations are labeled with text and color-coded using the same convention shown Figure 5 and ray diagrams shown in Figures 7a–7m. For plotting, an offset-varying gain has been applied to all receiver gathers. (a) Atka 1, (b) Atka 2, (c) OBS A2A3, (d) OBS A2C3, (e) Nikolski 2, (f) Fort Glenn 1, (g) Fort Glenn 2, (h) Chernofski, (i) Kashega, (j) Captain's Bay 2, (k) Beaver Inlet, (l) Akutan, and (m) Akun.

horizontally) observed in the final velocity model are reliable [*Van Avendonk et al.*, 2004].

8.1. Upper Crust

[22] Because of large minimum shot-receiver offsets (>20 km), the shallowest layer resolved by the wide-angle data lies at 5–11 km in depth. Refractions through this layer and reflections from the bottom of this layer are identified on nearly every instrument (Figures 6a–6m). All refractions are observed at shot-instrument offsets from the minimum offset recorded on each land instrument to as high as 75 km. Velocities range from 6.0 to

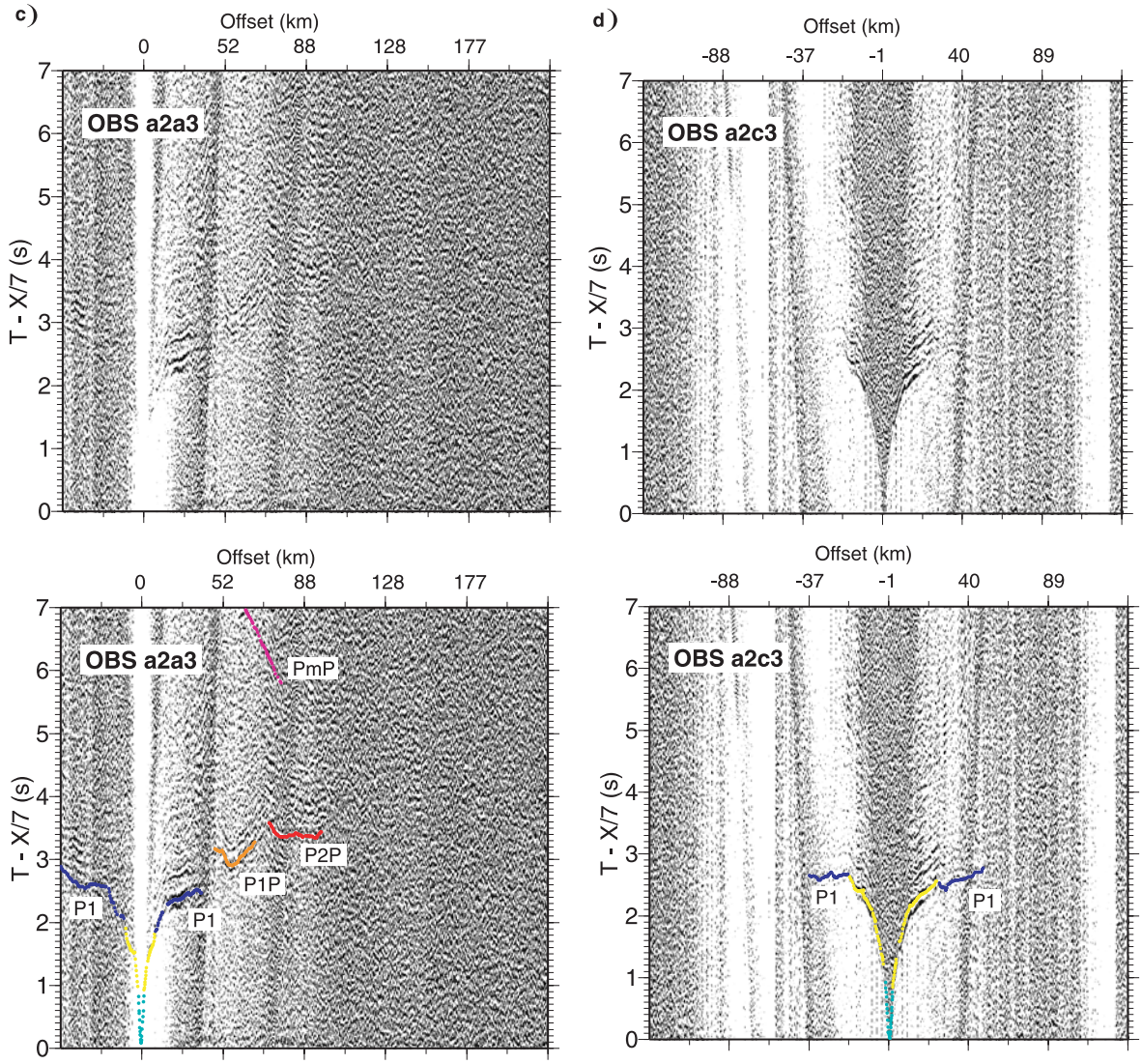

Figure 6. (continued)

6.5 km/s, with the highest velocities (6.5 km/s) observed at model km 350 and the lowest velocities (6.0 km/s) observed beneath Umnak Island at model km 475.

8.2. Middle Crust

[23] The middle crust is sampled by arrivals on eight receiver gathers and lies at depths of 10 to 20 km. Refractions from this layer consistently have apparent velocities close to 7 km/s (and appear flat on the reduced sections in Figures 6a–6m) and are typically seen from shot-instrument offsets of 70 to 150 km. Velocities in this depth interval range from 6.5 to 7.3 km/s, although the velocity variation is more modest in areas of dense ray coverage: 6.7–7.3 km/s. The highest velocities within the middle crust are found beneath Unalaska Island (model km ~620), and the lowest are found beneath the Islands of the Four Mountains (which include Kagamil, Chuginadak, Uliaga, Carlisle, and Herbert Islands, model km ~375).

8.3. Lower Crust

[24] The lower crust is the least constrained yet thickest crustal layer, extending from depths of ~20 to 35 km. PmP reflections and occasional direct arrivals require high velocities between 7.3 and 7.7 km/s. Direct arrivals are observed on five receiver gathers and span shot-receiver offsets of 140 to 180 km. Although lower-crustal refractions are rare in island arcs, they are also observed on lines A1 and A3 [*Holbrook et al.*, 1999; *Lizarralde et al.*, 2002]. The highest velocities within the middle crust are found beneath Umnak Island

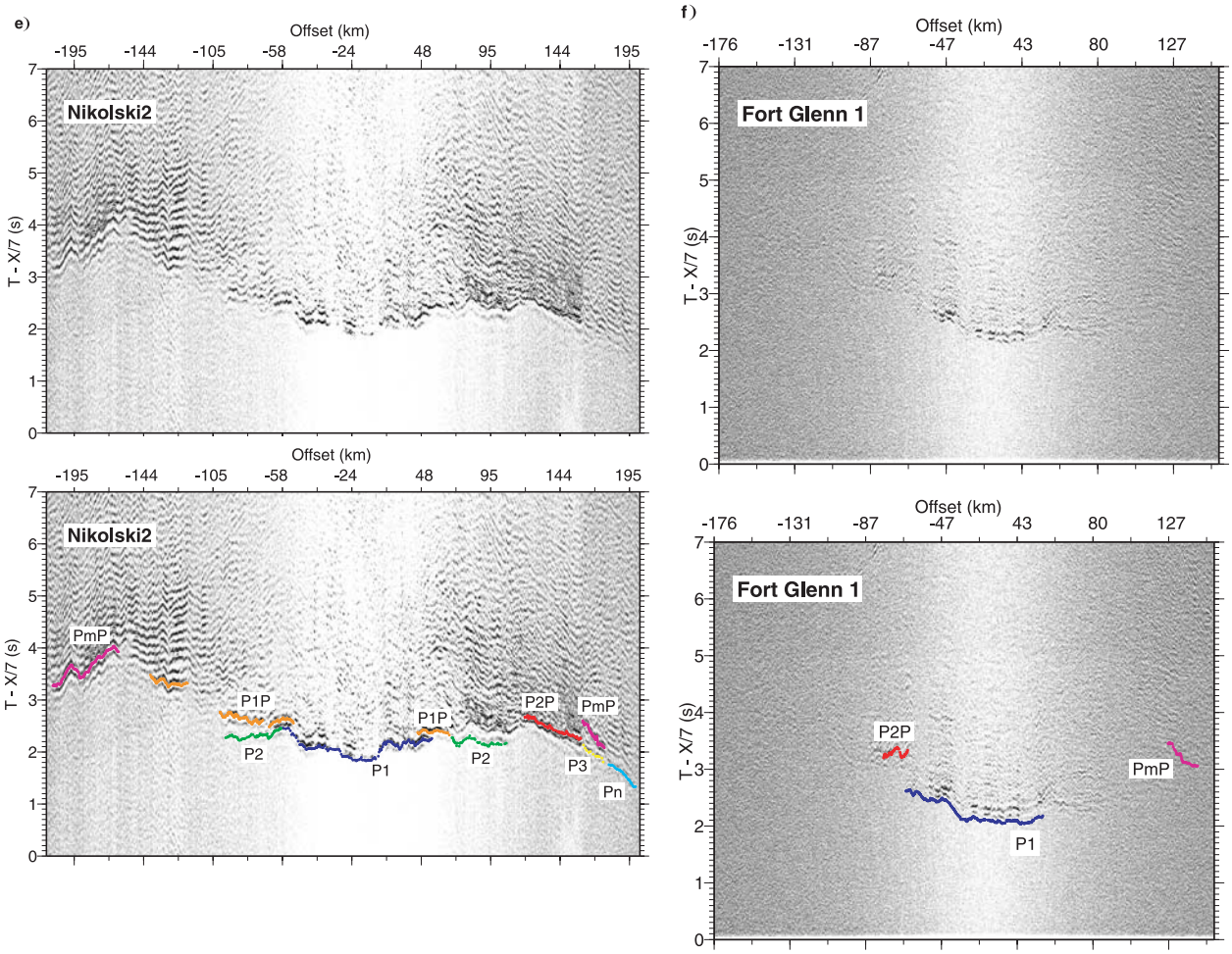

Figure 6. (continued)

(model km ~475), and the lowest velocities are found beneath Seguam Island (model km ~200) and Unimak Pass (model km ~725). We assume that the observation of lower-crustal refractions indicates increasing velocity with depth throughout the crust along line A2, and that no large or pervasive low-velocity zones are present in this region of the crust.

8.4. Uppermost Mantle

[25] Pn is rarely observed in this data set, only appearing on four instruments (Nikolski2, Kashega, Chernofski, and Captains Bay) for a short range of shot-receiver offsets (typically 180 to 190 km). Where seen, Pn gives upper mantle velocities of 7.8–8.1 km/s, significantly higher than observed in previous seismic investigations of this arc [*Fliedner and Klemperer*, 1999] or other arcs [*Hasegawa et al.*, 1991; *Zhao and Hasegawa*, 1994]. Picks on these instruments have the highest assigned errors (0.2 s) and worst fit in the final model [*Van Avendonk et al.*, 2004]. As a result, we have the least confidence in these interpretations and the mantle velocities derived from them.

8.5. Comparison With Other Seismic Velocity Models of Aleutians

[26] Below, we compare our velocity model for line A2 with previously published velocity models for line A2 [*Fliedner and Klemperer*, 1999, 2000], cross-arc lines A1 and A3 [*Holbrook et al.*, 1999; *Lizarralde et al.*, 2002], and the 3-D P wave velocity model in the eastern Aleutians derived from local earthquake arrivals by *Abers* [1994].

8.5.1. Previously Published Model of Line A2

[27] Our new velocity model differs in several significant respects from the velocity model previously published from this data set [*Fliedner and*

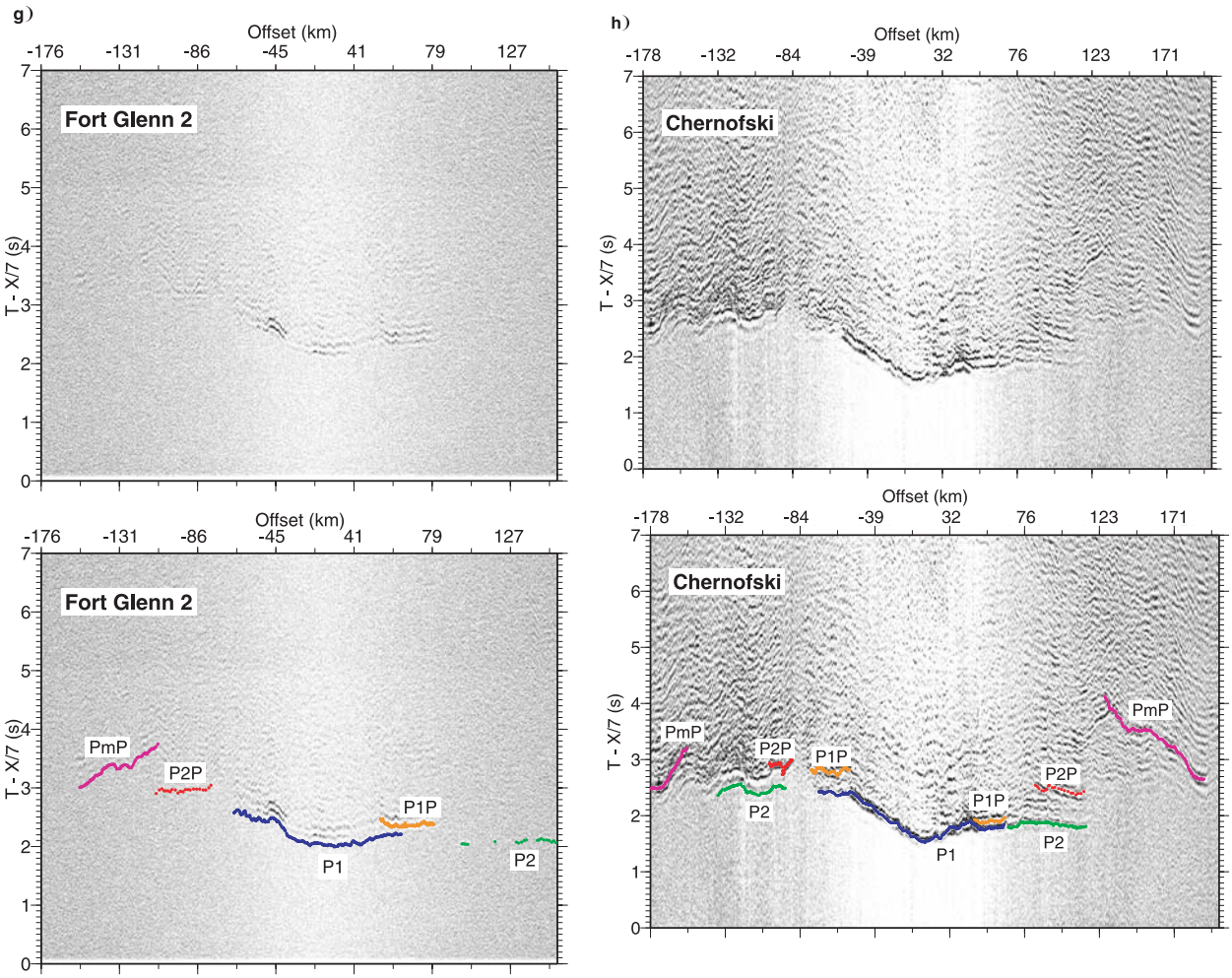

Figure 6. (continued)

Klemperer, 1999, 2000]: (1) higher velocities are observed in the middle and lower crust, (2) distinct vertical stratification of velocity structure is apparent, and (3) greater lateral continuity characterizes the middle and lower crust. While the model of *Fliedner and Klemperer* [1999] reaches comparably high velocities in the middle and lower crust (e.g., beneath Chernofski at FK model km ~475 and between OBS A2A3 and Nikolski at FK model km ~300), these do not persist across the length of the central Aleutians as they do in our model (Figure 9). For example, lower-crustal velocities as low as ~6.6 km/s are found beneath Akun Island in their model (FK model km ~625). Conversely, the lowest lower-crustal velocities found in our model are 7.3 km/s and lie in the vicinity of Seguam Island (model km 190). Given that the model of *Fliedner and Klemperer* [1999, 2000] has a thinner, lower velocity crust than our final model, we must assess the possibility that there might be a trade-off between lower crustal velocity and crustal thickness since this layer is the least constrained portion of the crust. *Van Avendonk et al.* [2004] calculate the trade-offs between lower crustal velocity and depth to the Moho and find maximum trade-offs of ~1 km in Moho depth and ~0.5 km/s in lower crustal velocity in the poorly constrained, westernmost portion of the model, and more typical tradeoffs of ~0.5 km in Moho depth and ~0.25 km/s in lower crustal velocity in the eastern part of the model, where data coverage is better. Since Fliedner and Klemperer find velocities as low as 6.6 km/s in the lower crust, these trade-offs cannot account for differences between our model and the model of Fliedner and Klemperer alone. Therefore the primary reason that our model is faster, overall, than the model of *Fliedner and Klemperer* [1999, 2000] is likely a difference in phase interpretations; middle and lower-crustal reflections and refractions interpreted on many instruments (Figures 6a–6m) require high velocities in these layers.

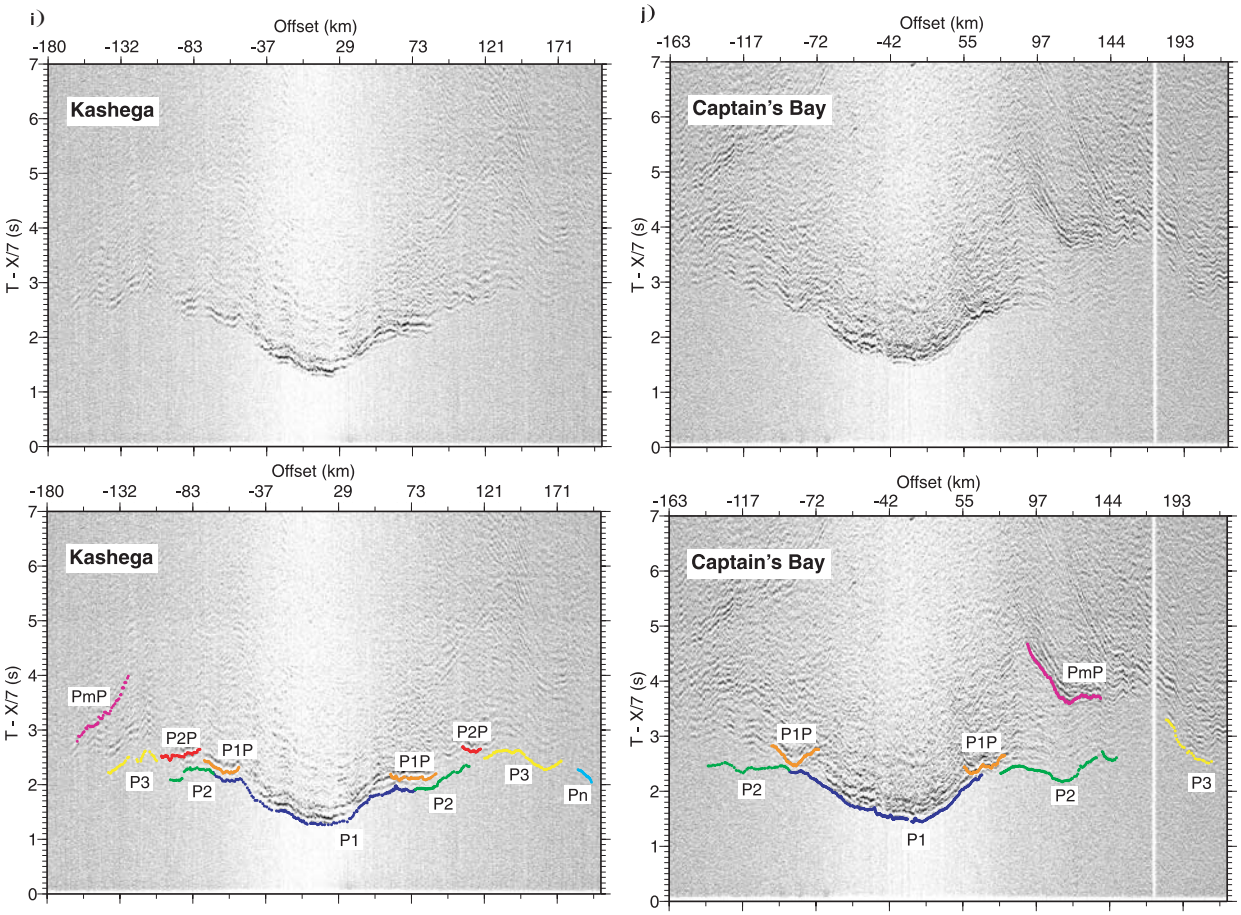

Figure 6. (continued)

[28] In addition to the higher velocities observed in our model, the models differ in their horizontal and vertical structure. The model presented in this paper is more vertically stratified, containing three layers, separated by velocity discontinuities; this is a direct consequence of our phase interpretations, which recognize refractions from each layer bound by reflections off of the boundaries between layers, and of our resulting modeling parameterization [*Van Avendonk et al.*, 2004]. In contrast, the model of *Fliedner and Klemperer* [1999] does not show similar stratification; they interpreted intracrustal reflections as "floating" within a continuous velocity layer rather than indications of velocity boundaries [*Hole*, 1992; *Fliedner and Klemperer*, 1999].

[29] Both models have some degree of lateral variability, though its manifestation in our model is more subdued. Our model shows variations of ~0.4 km/s in the lower crust; *Fliedner and Klemperer* [1999] have ~0.8 km/s. We attribute the mitigation of some small-scale lateral variability in our model to our incorporation of shallow velocity structure, which explains some of the small-scale structure observed in crustal phases on wide-angle records (Figure 3). Our use of 2.5-D inversion rather than a 3-D inversion for this sparse data set and our choice of smoothing parameters would likely result in a more constrained and smoother final model with fewer dramatic lateral variations.

8.5.2. Lines A1 and A3

[30] Substantial differences and similarities can also be observed between cross-arc lines A1 and A3 [*Holbrook et al.*, 1999; *Lizarralde et al.*, 2002]. A similar three-layer structure is observed in these models; this might be partially due to the similar approach to phase interpretation employed by these authors. However, these models differ from line A2 in that they show thinner crust and lower velocities in the middle and lower crust. Line A1, which crosses the western portion of line A2 between Seguam and Amlia Islands, reaches a maximum

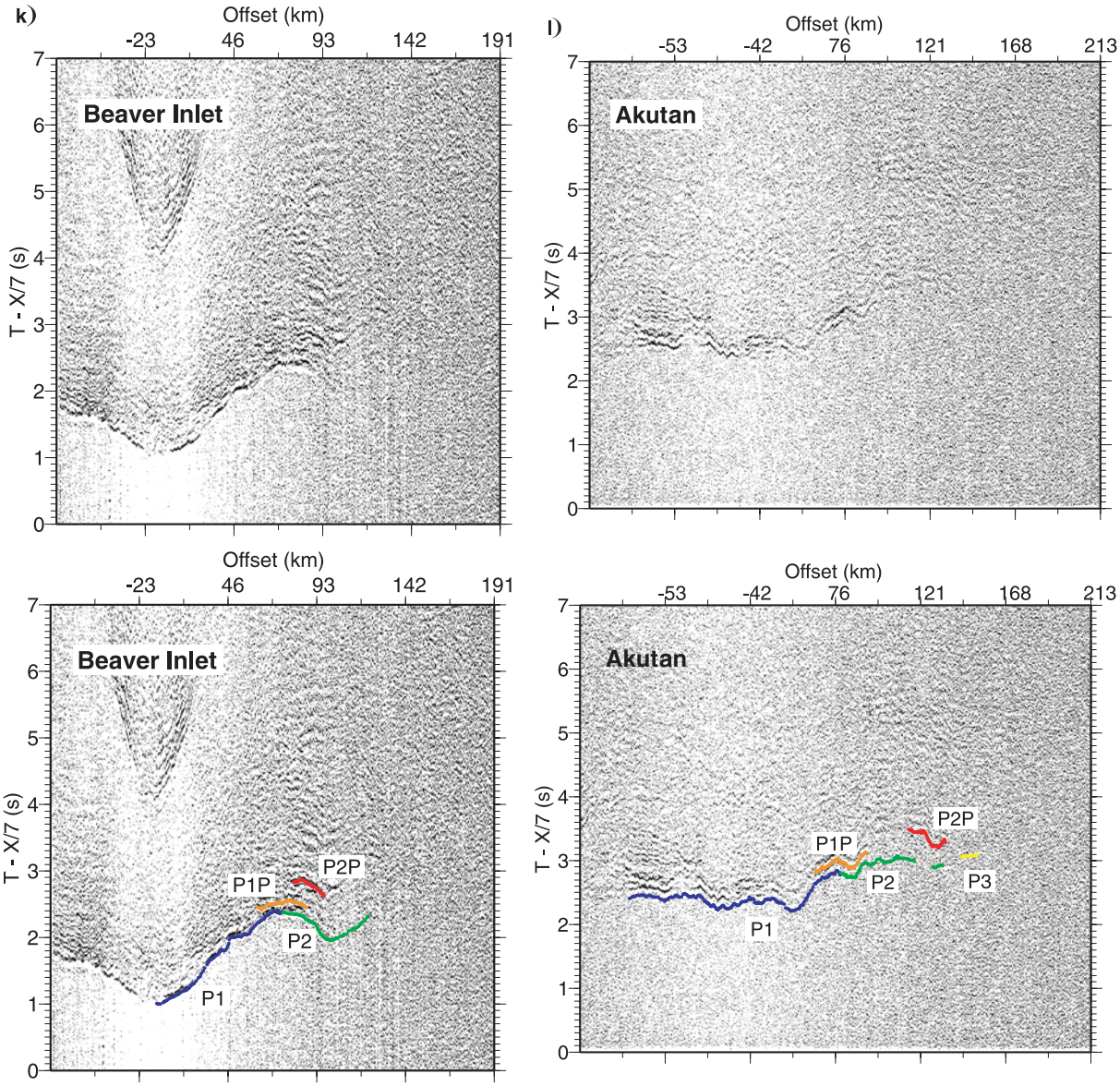

Figure 6. (continued)

thickness of ~30 km and contains middle-crustal velocities of 6.6–6.8 km/s and lower-crustal velocities of 7.0–7.3 km/s. Our velocity model is slightly faster and thicker at this crossing, with middle-crustal velocities of ~6.8 km/s, lower-crustal velocities of ~7.3 km/s, and a crustal thickness of 35 km (model km ~180 km, Figure 8). Line A3, which crosses the eastern portion of line A2 at Unimak Pass (model km ~750, Figure 8), intersects a complicated portion of line A3, where lower-crustal velocities are laterally increasing from 6.9 to 7.4 km/s, and at the edge of a thick portion of middle crust, which *Lizarralde et al.* [2002] attribute to tectonic thickening of the Kula plate. At the intersection, line A3 contains middle-crustal velocities of ~6.8 km/s, lower-crustal velocities of ~7.0–7.3 km/s, and a crustal thickness of 32 km. Once again, line A2 has a slightly thicker crust and higher velocities, with middle-crustal velocities of 6.9–7.0 km/s, lower-crustal velocities of 7.3–7.4 km/s and a crustal thickness of 35 km. However, these portions of the line A2 model are poorly resolved; they are crossed only by ray paths recorded by instruments positioned on Atka and on Akutan and Akun, respectively, which show comparatively poor data quality (Figures 6a, 6b, and 8b).

[31] The comparatively high velocities and thick crust on line A2 might be explained by the influence of the forearc. While most of the ray paths

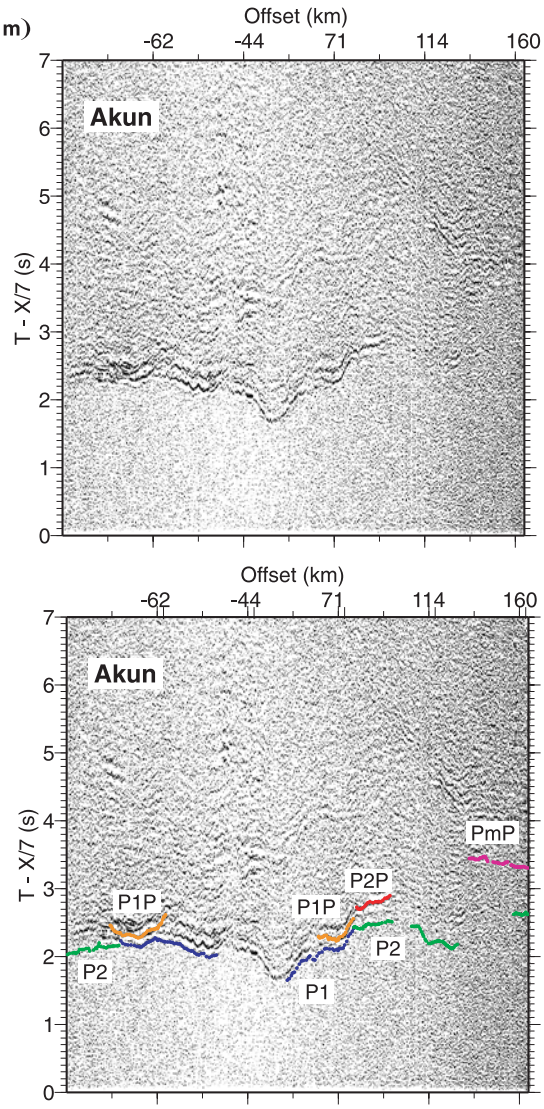

Figure 6. (continued)

used in the creation of the line A2 model lie on the trenchward side of the arc platform (~20 km from the active volcanic line), a small proportion of the ray paths traverse what appears to be a transition from forearc to arc crust in the cross-arc lines (Figure 4). The forearc on both lines A1 and A3 is composed of material with higher middle- and lower-crustal velocities compared to the arc. Additionally, lines A1 and A3 intersect the extremities of line A2, and are thus only crossed by unreversed phases. As a result, these portions of the model are poorly constrained.

8.5.3. Velocity Model From Local Earthquakes

[32] A 3-D velocity model for the eastern Aleutians around Unimak Island and the Alaska Peninsula has also been derived using P and S waves generated by local earthquakes [*Abers*, 1994]. This model contains comparatively high velocities at depths of ~20–35 km beneath Unimak Island. Lower-crustal velocities beneath the arc at Unimak Island range from 7.39–7.90 km/s, which compare well with lower-crustal velocities on line A2 (7.3–7.7 km/s). Likewise, middle-crustal velocities in this model are ~6.3–7.29, which are also similar to those observed on line A2 (6.5–7.3 km/s). As in cross arc lines A1 and A3, earthquake arrivals also indicate that crustal velocities generally increase southward approaching the forearc [*Abers*, 1994; *Holbrook et al.*, 1999; *Lizarralde et al.*, 2002].

9. Discussion

[33] Our final velocity model contains several new features that bear on arc composition and structure: (1) relatively high middle- and lower-crustal velocities, (2) distinct three-layer structure, (3) a correlation between lower-crustal velocities and arc segmentation, and (4) along-arc variations in average velocity that correspond to trends in extrusive geochemistry. Velocities in the middle (~6.92 km/s) and lower crust (~7.45 km/s) suggest the predominance of mafic material in the Aleutian island arc (Figure 8).

9.1. Considerations for Interpreting Velocity Structure

[34] In the following sections, we seek to link seismic velocity to the composition of arc-related magmatic additions. However, the interpretations made from our velocities will depend on the thermal gradient structure of the arc and on the velocity structure of the crust on which the Aleutian island arc is built. We briefly describe each of these additional considerations in this section.

[35] Our choice of a thermal gradient will affect the temperature corrections applied to laboratory measurements for comparison with our data. Many reviews have been completed of arc thermal structure. Here, we seek a reasonable range of geothermal gradients that would apply to the crust beneath line A2. Because line A2 lies ~20 km trenchward of the active volcanic line, we anticipate a cooler geothermal gradient here than beneath the active volcanic line itself. Many recent studies indicate a sharp gradient in arc temperatures in this area [*Hyndman and Peacock*, 2003]. For example, the thermal models of *Hyndman and Peacock* [2003] can be used to show a drop in the geothermal

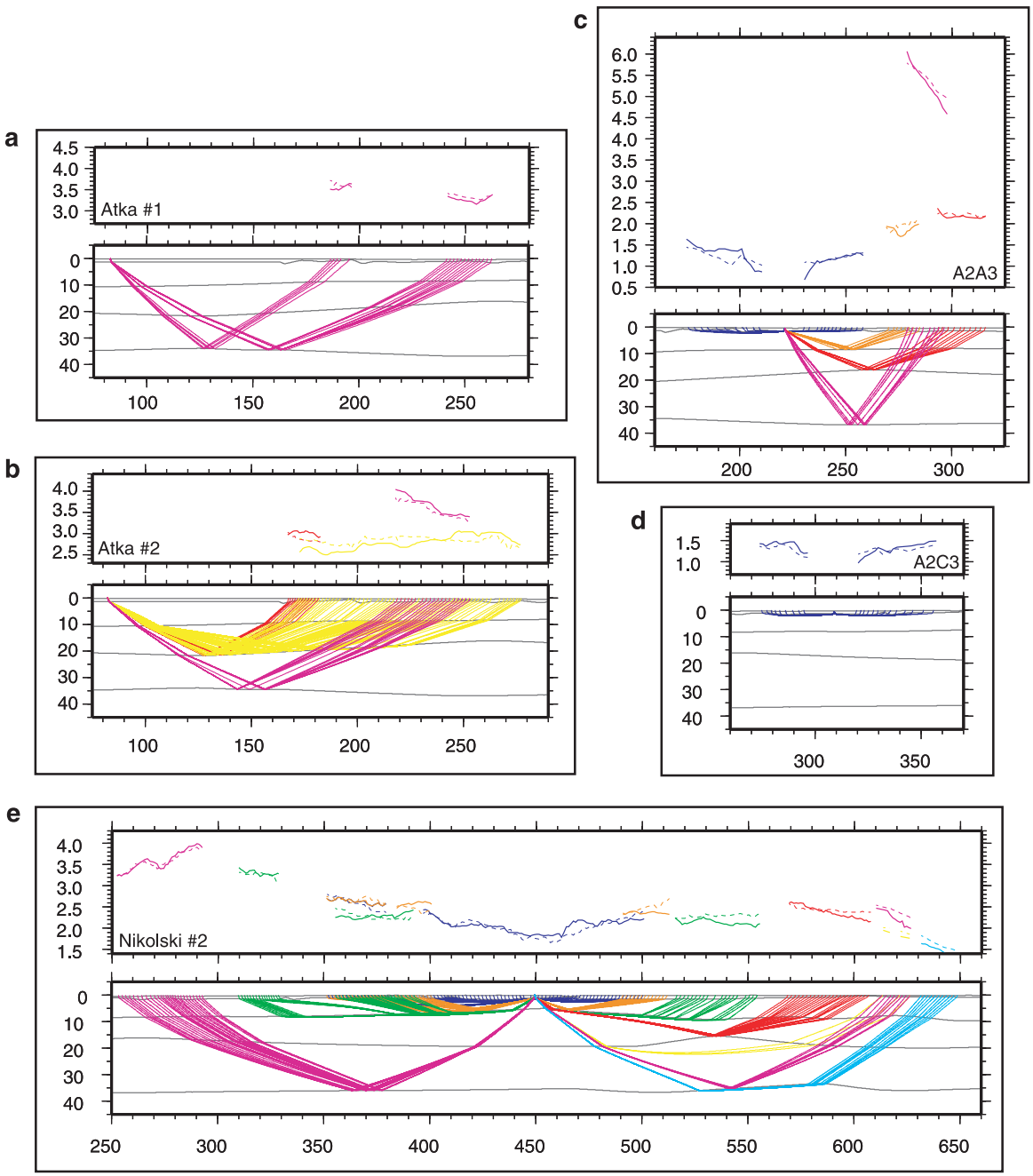

Figure 7. Model predictions and picks from each receiver gather used in model creation. Picks are shown as solid lines, and model predictions are shown as dashed lines. Picks and predictions are color-coded by phase, consistent with Figures 5 and 6a–6m. (a) Atka 1, (b) Atka 2, (c) OBS A2A3, (d) OBS A2C3, (e) Nikolski 2, (f) Fort Glenn 1, (g) Fort Glenn 2, (h) Chernofski, (i) Kashega, (j) Captain's Bay, (k) Beaver Inlet, (l) Akutan, (m) Akun.

gradient from 20°C/km to 15°C/km by moving 20 km trenchward of the active arc in NE Japan, which is similar to the Aleutians in that cold, old oceanic crust is subducting in this trench. Since our line lies in the vicinity of this lateral change in the thermal regime, we correct experimental velocities for temperature using both 15 and 20°C/km, although the location of our line and the high velocities in our model, which imply cooler temperatures, lead us to favor the cooler gradient.

[36] Knowledge regarding the crust on which the Aleutian arc is built is critical when considering the composition and volume of arc magmatic products. Most of the Aleutian island arc sampled by line A2 is built on oceanic crust, likely from the relic Kula

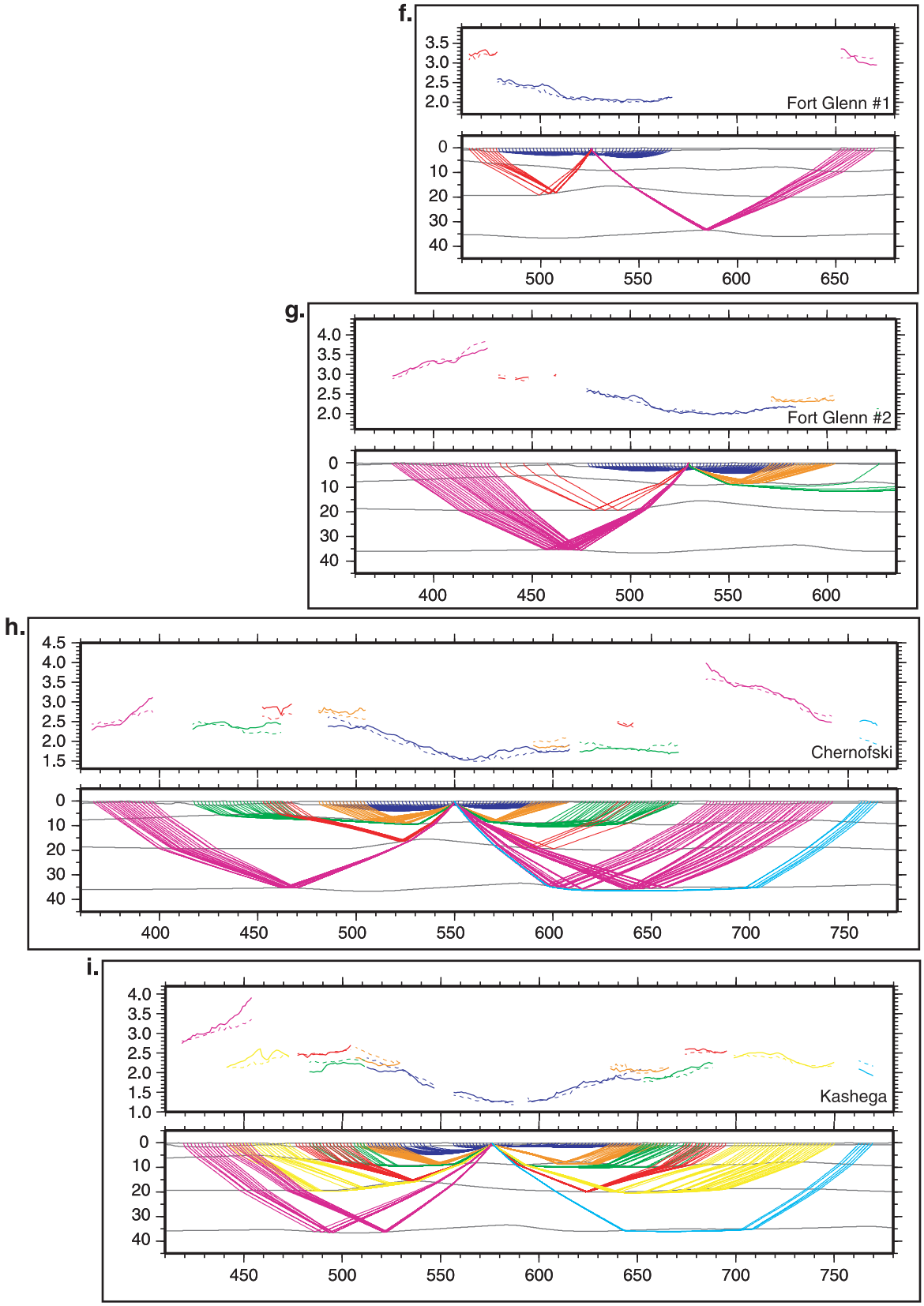

Figure 7. (continued)

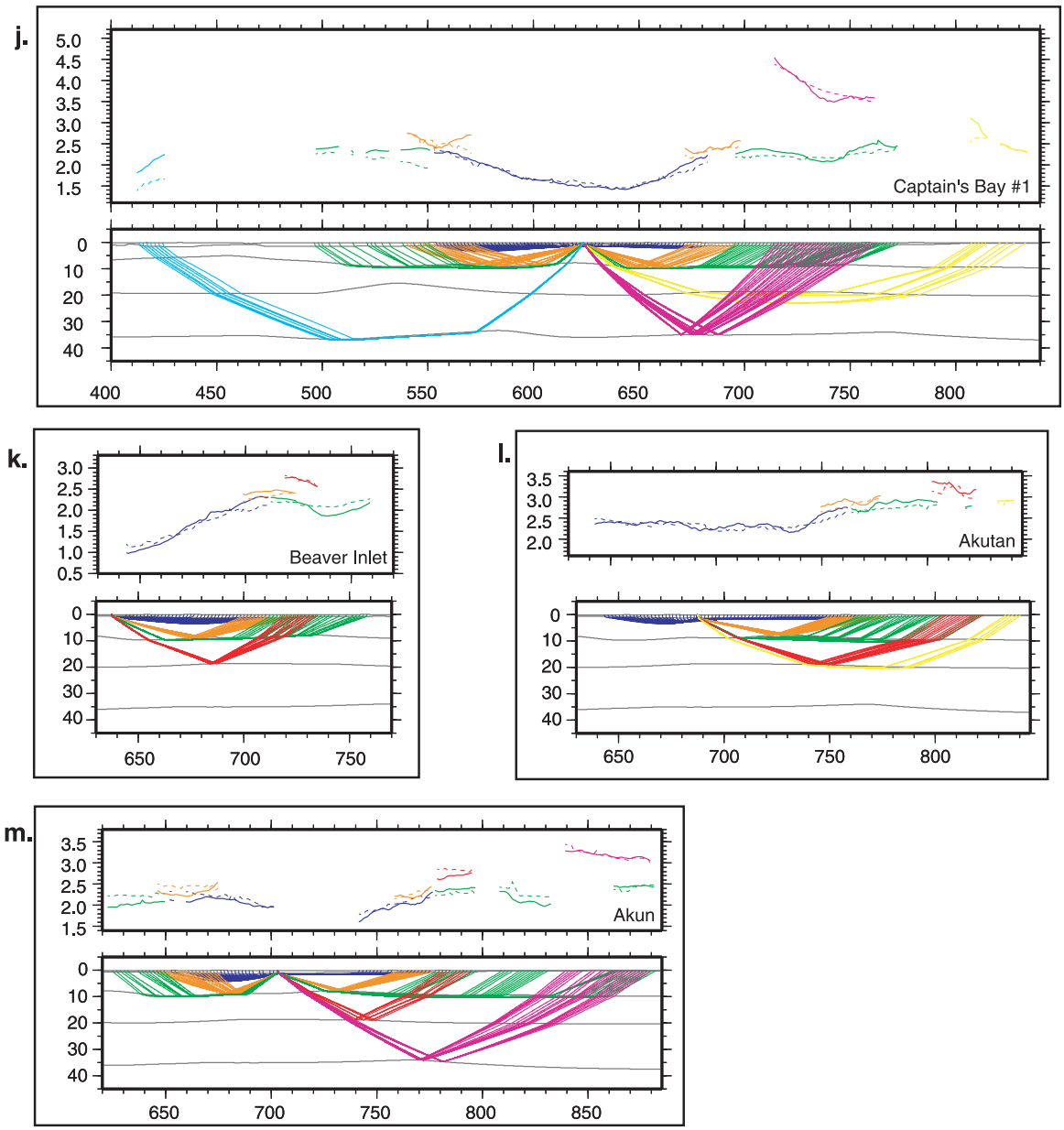

Figure 7. (continued)

plate. In these places, as much as 5 km of the Aleutian midcrust might be attributed to oceanic crust [*Lonsdale*, 1988]. Lines A1 and A3, cross-arc lines that intersect line A2 at Seguam Pass and at Unimak Pass (Figure 1), image a ~5-km thick layer with velocities of ~6.5–6.9 km/s, which have been interpreted to represent oceanic crust [*Holbrook et al.*, 1999; *Lizarralde et al.*, 2002]. Near the intersection with line A2, *Lizarralde et al.* [2002] interpret a 10-km-thick bulge with velocities of 6.7–6.9 km/s on line A3 to represent tectonic thickening of the Kula plate. Part of the Aleutian island arc beneath line A2 passes south of Unmak Plateau, which might be an oceanic plateau that was added to Alaska contemporaneously with the Kula plate [*Ben-Avraham and Cooper*, 1981] (labeled on Figure 1). If this section of the Aleutian island arc is indeed built on an oceanic plateau, the original velocity structure of the crust on which the Aleutian arc was built might be very different from "normal" oceanic crust. For example, seismic studies of the Ontong Java oceanic plateau yield crustal thicknesses of 31 km and a three layer structure with middle-crustal velocities of 6.1 km/s and lower-crustal velocities of 7.1 km/s [*Gladczenko et al.*, 1997]. Other oceanic plateaus

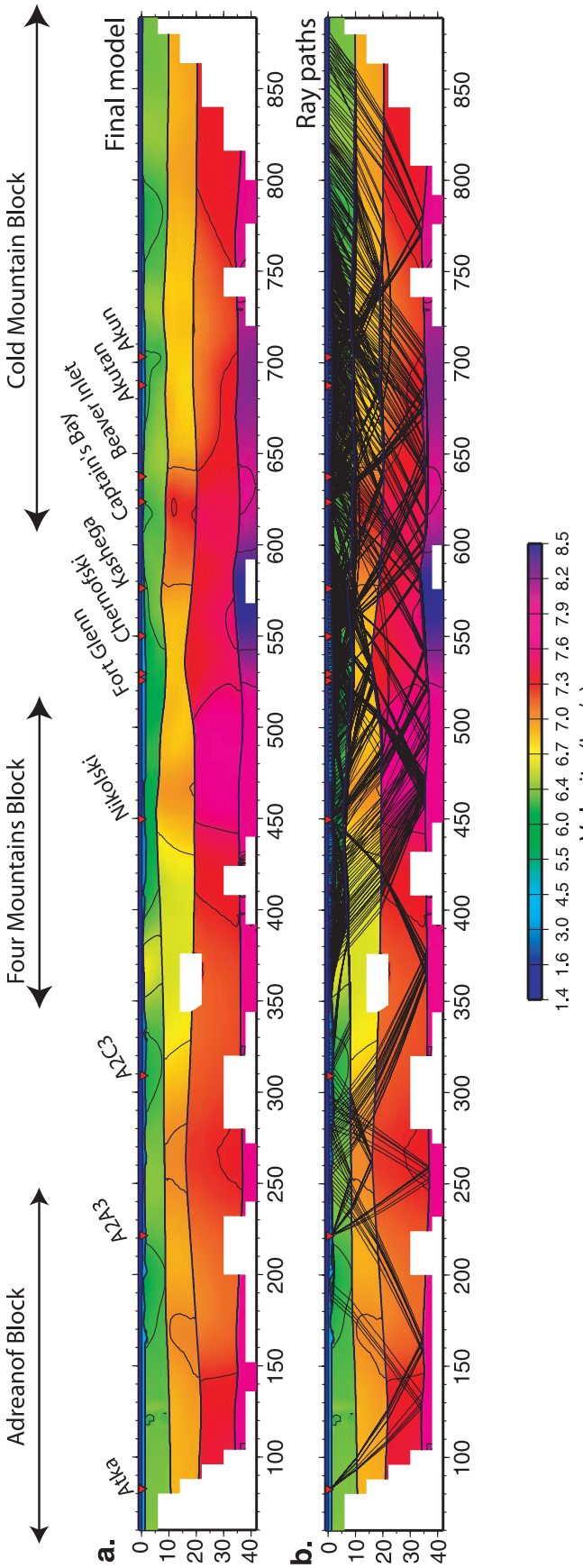

Figure 8. (a) Final P wave velocity model. (b) Final velocity model with projection of 3-D ray paths on vertical plane used for model construction.

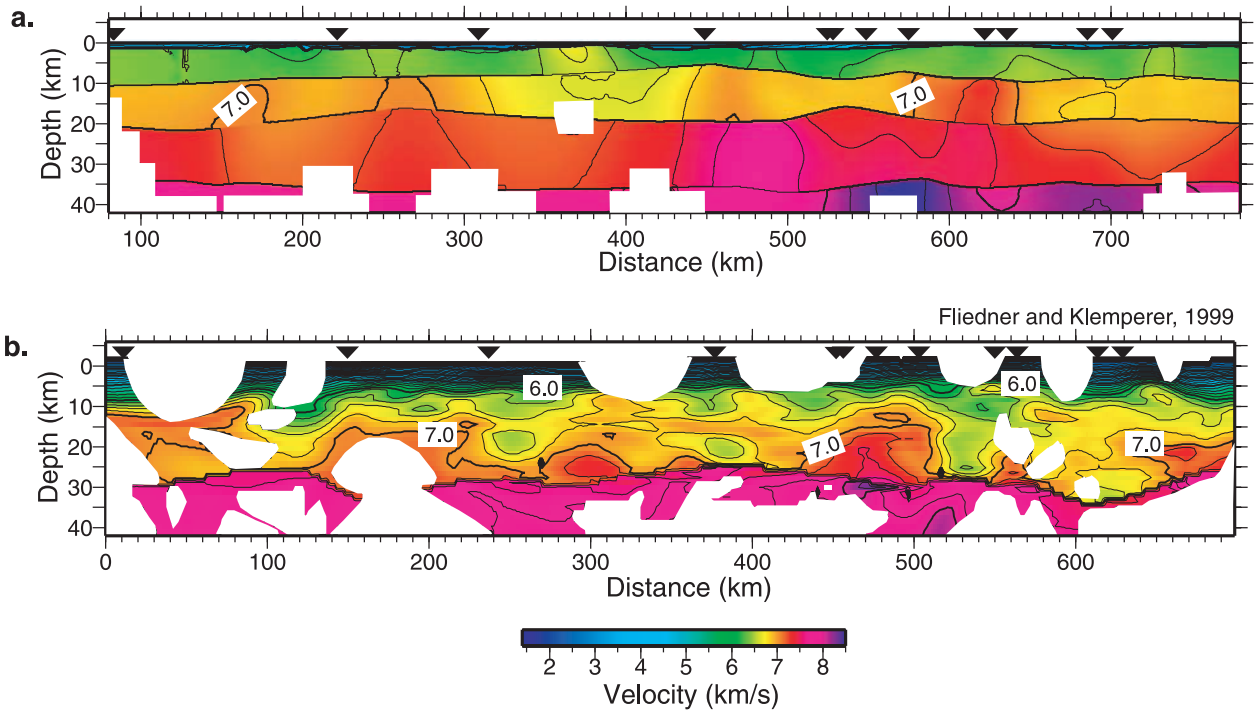

Figure 9. Comparison of (a) final velocity model to (b) previously published model of *Fliedner and Klemperer* [1999, 2000]. Please see text for comparative description of models. Figures 9a and 9b are plotted with the same color scale and a contour interval of 200 m/s.

show variable thicknesses and velocity structures [*Ben-Avraham and Cooper*, 1981]. Because of the uncertainties associated with the creation and amalgamation of the Umnak Plateau, including its original thickness and velocity structure, it is impossible to quantify the extent to which it accounts for middle and lower crustal velocity structure in this area. Consequently, we assume that the Aleutian island arc along line A2 was primarily built on oceanic crust in our discussion of the middle crust.

9.2. Upper Crust Composition

[37] Upper-crustal velocities of 6.0–6.5 most likely indicate the presence of fractured plutonic rocks and, to a lesser extent, volcanic flows [*Holbrook et al.*, 1999; *Lizarralde et al.*, 2002]. The depth range of this layer allows lateral velocity variation to be explained by either variable composition or by fracture and porosity distribution, as cracks are found in the earth at depths up to 12 km [*Carlson and Gangi*, 1985; *Ganchin et al.*, 1998]. Thus it is impossible to determine composition at these depths from seismic velocity. The major element geochemistry of rocks exposed at the surface suggests that diverse compositions would be present in this layer; basaltic lavas are most abundant in the central Aleutian Islands [*Myers*, 1988], while exposed plutonic rocks in the same region are most often andesitic [*Kelemen*, 1995; *Kelemen et al.*, 2003a].

9.3. Middle Crust Composition

[38] Middle-crustal velocities between 6.5–7.3 km/s permit a wide range of possible compositions, although the spectrum of velocities in well-resolved portions of the model is more limited: 6.8–7.3 km/s (Figure 8b). We interpret these velocities to represent a combination of mafic and intermediate plutons that been added to the oceanic crust on which most the central Aleutians was constructed. Despite the large range of velocities and implied permissible compositions, the average middle-crustal velocity of 6.92 km/s in this depth range indicates that the middle crust of this arc is relatively mafic compared to other arcs and continental crust. We briefly review outcrop and xenolith studies in the Aleutians, studies of the middle crust of obducted arcs, and experimental and theoretical calculations of middle-crustal composition and velocity, and we compare these to middle-crustal velocities in the central Aleutians.

[39] As described in the previous section, we attribute some of the middle crust (~5 km) to

the oceanic crust on which the Aleutian island arc is built. Intrusive arc magmatic products must account for the additional thickness of the middle crust on line A2 (~5 km). The majority of exposed plutonic rocks in the Aleutians, unlike the extrusive rocks, have an average composition equivalent to an andesite [*Kelemen*, 1995; *Kelemen et al.*, 2003a]. Although it is uncertain how representative these might be of more remote middle-crustal material, their presence in outcrop and the likelihood that rising andesitic magmas are more viscous than their basaltic counterparts, and are thus more likely to crystallize in the middle crust than erupt at the surface, suggest that they may be abundant in this depth interval [*Kelemen*, 1995; *Kelemen et al.*, 2003a]. Very few samples of middle-crustal origin have been recovered in the Aleutians with which we might compare middle-crustal velocities on line A2, and these are very diverse, ranging from granites to gabbronorites. *Conrad and Kay* [1984] inferred that hornblende gabbro xenoliths represent the most common midcrustal composition beneath Mt. Moffet on Adak Island, but they had little basis for deciding if a xenolith came from the middle or lower crust.

[40] Comparatively low velocities observed in the middle crust in some parts of our model (e.g., <6.8 km/s at model km ~375 beneath Four Mountain Islands) strongly imply intermediate compositions, as they are too low to represent gabbros [*Korenaga et al.*, 2002]. Global compilations of P wave velocities for gabbros (6.954–7.118 km/s for depths of 10–20 km and temperatures of 116°–501°C) [*Christensen and Mooney*, 1995] and more recent calculations using elastic constants for minerals, and mixture theory to calculate gabbroic rock velocities [*Korenaga et al.*, 2002] indicate that high velocities (>7.1 km/s) in other sections of the middle crust unambiguously suggest the presence of gabbroic plutons. Recent estimations of velocity based on mineral assemblages predicted at middle-crustal depths by thermodynamic calculations allow for between 48.5 to 62.3 wt% SiO_2 and 4.2 to 7.8 wt% MgO for an average continental geothermal gradient (q_s = 56 mW m^{-2}), equivalent to the geothermal gradients discussed earlier [*Behn and Kelemen*, 2003].

[41] The presence of both andesitic and basaltic compositions in the middle crust is consistent with the composition and velocity of middle-crustal rocks collected from obducted arcs (e.g., Kohistan, Pakistan and Talkeetna, AK, USA), which are predominantly gabbroic in most descriptions [*DeBari and Coleman*, 1989; *Pearcy et al.*, 1990; *Miller and Christensen*, 1994] but also contain large, felsic intrusive units [*Khan et al.*, 1989; *Krol et al.*, 1996; *Kelemen et al.*, 2003a; A. R. Green et al., A detailed geochemical study of island arc crust: The Talkeetna Arc Section, south-central Alaska, submitted to the *Journal of Petrology*, 2003 (hereinafter referred to as Green et al., submitted manuscript, 2003)]. *Miller and Christensen* [1994] report V_p of middle-crustal samples from Kohistan measured at middle-crustal confining pressures at values between ~6.7–7.6 km/s, excluding a thin dunite layer. Measured samples interpreted to be midcrustal in origin include hornblende gabbronorites, gabbronorites, olive gabbros, and amphibolites. Once corrected for temperature using the dV_p/dT (km/s/°C) values of 3.6×10^{-4} for fractionated crystal assemblages with velocities of 6.7 km/s and of 4.7×10^{-4} for assemblages with velocities of 7.6 km/s [*Korenaga et al.*, 2002], expected velocities range from 6.6 to 7.5 km/s for a geothermal gradient of 15°C/km and 6.5 to 7.4 km/s for a geothermal gradient of 20°C/km. These velocities are comparable to those in the middle crust of our velocity model. In summary, we interpret middle-crustal velocities of 6.5–7.3 km/s to represent plutons of andesitic to basaltic composition that have intruded the oceanic crust on which the central Aleutians are built. Although this range of velocities allows a wide range of permissible middle-crustal compositions, it still has a higher velocity than average continental midcrust (6.31 ± 0.27 at 15 km, 6.47 ± 0.28 at 20 km) [*Christensen and Mooney*, 1995] and other island arcs (~6.0 km/s) [*Suyehiro et al.*, 1996] at comparable depths.

9.4. Lower Crust Composition

[42] High lower-crustal velocities of 7.3–7.7 km/s suggest that the lower portion of the central Aleutian island arc is composed primarily a mixture of garnet-bearing rocks, gabbros and ultramafic rocks. Below, we briefly review studies of xenoliths from the lower crust of the Aleutian island arc, materials commonly found in the lower-crustal sections of obducted arcs, and materials predicted by fractionation models and crystallization experiments, and we compare the velocities of these materials to velocities observed in the lower crust of our model. We also discuss the possible contribution of garnet to high lower-crustal velocities.

[43] Xenolith and geophysical studies in the Aleutian island arc provide corroboration for our interpretation of lower-crustal velocities.

Mafic-ultramafic cumulates originating in the lower crust and upper mantle have been recovered from Adagdak and Moffet volcanoes, Adak [*Conrad and Kay*, 1984; *DeBari et al.*, 1986]; these include dunites, clinopyroxenites, wehrlites and amphibolites. *Holbrook et al.* [1999] correlate high lower-crustal velocities on line A1, which intersects line A2 at Seguam Pass, as mafic residua resulting from either calc-alkaline or tholeiitic fractionation. *Lizarralde et al.* [2002] also interpret high lower-crustal velocities under the arc on line A3 to represent mafic cumulates.

[44] Obducted arcs often preserve lower-crustal sections to which we can compare lower-crustal velocities of the central Aleutians along line A2. These sections are typically thin and may have lost material via delamination or during tectonic exhumation; thus they might not be representative of the original lower crust compositions or abundances [*Jull and Kelemen*, 2001; *Kelemen et al.*, 2003a]. Velocity measurements of samples of mafic cumulates from the lower-crustal section of the Kohistan accreted arc taken at lower-crustal confining pressures found V_p values between ~7.4–8.1 km/s [*Miller and Christensen*, 1994]. These samples included amphibolites, garnet-bearing (30–35%) gabbros, garnet-bearing (~35%) hornblendites, serpentinized olivine pyroxenites, and websterites. Correcting for the effects of temperature using the relationship between velocity and dV_P/dT for fractionated crystal assemblages of 5.6×10^{-4} (km/s/°C) derived by *Korenaga et al.* [2002] yields a velocity range of 7.2 to 7.8 km/s for a geothermal gradient of 15°C/km and 7.1 to 7.7 km/s for a geothermal gradient of 20°C/km. The depth range of our lower crust (~20–35 km) is consistent with depth estimates of lower-crustal cumulates from the Tonsina ultramafic and mafic assemblage based on phase relationships, which yield depths of 28–33 km (9.5–11 kbar) and temperatures of 800 to 1000°C [*DeBari and Coleman*, 1989; *Kelemen et al.*, 2003b]. *Pearcy et al.* [1990] also estimate that basal cumulates in the Canyon Mountain arc complex formed between 15–30 km.

[45] Finally, global compilations and experimental data also support this interpretation of high lower-crustal velocities. *Christensen and Mooney* [1995] report velocities of 7.407–7.739 km/s for a pyroxenite at combinations of pressures suitable for depths between 20–35 km and temperatures between 309°–925°C. For the same range of depths and temperatures, *Christensen and Mooney* [1995] measured velocities of 6.788–7.120 km/s for hornblendites and 6.769–7.106 km/s for gabbro norite troctolites. A mixture of such compositions could produce the observed velocities. Likewise, velocities determined for a range of igneous compositions using thermodynamic calculations allows compositions with wt% SiO_2 between 44.8 and 49.5 and wt% MgO between 12.7 and 14.6 for an average continental geothermal gradient, equivalent to those discussed in a previous section.

[46] The extent to which garnet contributes to observed high velocities in the lower crust is uncertain. Because garnet-bearing metamorphic rocks, derived from intermediate to mafic plutonic rocks, are common in lower-crustal arc assemblages [*DeBari and Coleman*, 1989; *Miller and Christensen*, 1994; *Jull and Kelemen*, 2001; *Kelemen et al.*, 2003a], we infer that they are likely to be present in the Aleutian lower crust. Depending on bulk composition and H_2O content, garnets can be stable in primitive gabbroic bulk compositions at lower-crustal temperatures and at pressures greater than 1.0 GPa, and at pressures greater than 0.7 GPa for more evolved gabbroic and dioritic compositions (high Fe/Mg) [*Johnson and Essene*, 1982; *Jull and Kelemen*, 2001; *Müntener et al.*, 2001]; most of the lower crust in this model resides below 20 km, the approximate depth at which garnets may begin to form in some (Fe-rich) compositions.

[47] Phase equilibria calculations suggest that the formation of abundant garnet occurs over a narrow pressure interval once garnet becomes stable in a given bulk composition [*Jull and Kelemen*, 2001]. This could produce a velocity discontinuity or high velocity gradient at the garnet isograd in compositionally uniform lower crust. However, sharp increases in garnet distribution over a narrow depth range are not expected within a compositionally heterogeneous lower crust. Thus the sharp middle- to lower-crustal boundary in our model could be due to the garnet isograd in compositionally uniform, relatively evolved intermediate to mafic plutonic rocks, or to an abrupt change in bulk composition between the two layers. In summary, high velocities in the lower crust of our model suggest a mixture of mafic and ultramafic cumulates; we also conclude that garnets are likely present in these assemblages and probably contribute to the observed high velocities.

9.5. Upper Mantle Composition

[48] Our upper mantle velocities of 7.8–8.1 km/s are somewhat high for the uppermost mantle of an

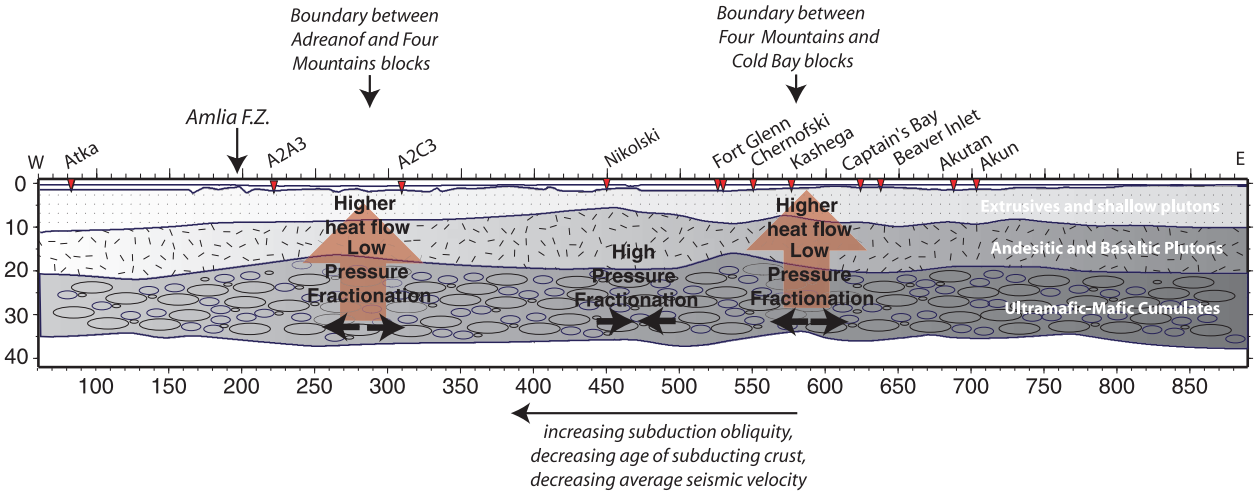

Figure 10. Cartoon illustrating the interpretation of the middle and lower crust. In this interpretation, high lower-crustal velocities found in the eastern portion of the model and in the center of a structural block are the result of cooler temperatures and relatively high pressure fractionation, which is expected to produce comparatively felsic extrusives at the surface and leave correspondingly mafic cumulates in the lower crust [*Kay et al.*, 1982]. Likewise, lower-crustal velocities are relatively low at segment edges because of elevated temperatures caused by rising warm material [*Singer and Myers*, 1990] and by the comparatively less mafic cumulates generated by low-pressure fractionation, which is anticipated at structural block edges [*Kay et al.*, 1982]. Black arrows represent the stress regimes predicted at segment edges and in segment centers. On a larger scale the average velocity of the crust steadily decreases westward, possibly because of the increasing obliquity of subduction or the decreasing age of the subducting plate; this is illustrated with the thin black arrow at the base of the cartoon.

island arc. Previous studies (including the previous study of this data set) record velocities as low as 7.6 km/s [e.g., *Fliedner and Klemperer*, 1999]. Low velocities in other studies have been used to suggest the presence of partial melt and/or very high temperatures in the uppermost mantle [*Kelemen et al.*, 2003b]. The presence of relatively high velocities beneath the central Aleutians is likely attributed to the location of line A2, 20 km trenchward of the active volcanic line, where fewer partial melts would be expected. It might also suggest that the uppermost mantle here, where sampled by turning waves in this experiment, is composed of ultramafic cumulates, similar to those observed beneath the Moho in the Kohistan and Talkeetna obducted arcs [*DeBari and Coleman*, 1989; *Pearcy et al.*, 1990; *Miller and Christensen*, 1994; *Müntener et al.*, 2001; *Kelemen et al.*, 2003a] and to ultramafic xenoliths recovered in the Aleutians with depths of origin estimated below the Moho [*Kay and Kay*, 1985; *DeBari et al.*, 1986]. Finally, Pn is likely only found in our data set where there is a sufficient contrast between the lower crust and upper mantle; particularly because we detect high lower-crustal velocities here, our sampling might be biased toward the highest mantle velocities. Because Pn samples only a small percentage of the upper mantle under the Aleutians and has poor travel time fits, these velocities may not be representative.

9.6. Compositional and/or Mineralogical Stratification

[49] The velocity model presented in this paper contains three distinct velocity layers within the crust, which extend across the entire 800 km span of line A2. This vertical stratification is a direct consequence of our phase interpretations, which identify three distinct crustal refractions, bound by reflections. Although such a pattern is observed on nearly all instruments where data quality permit, bounce points on layer boundaries do not require this structure continuously across the entire arc (Figure 8b). However, if present, such velocity structure most likely represents compositional stratification, particularly at the upper- to midcrust boundary. The middle- to lower-crustal boundary could be produced either by a compositional transition or a sharp gradient in the modal proportion of garnet within compositionally homogeneous rocks, as the interpretations of velocities within each of these layers given above suggests (Figure 10). The implied existence of laterally

continuous stratification within the Aleutian island arc is consistent with studies of active arcs, which infer discrete compositional layers within arcs based on fractionation models [*Conrad and Kay*, 1984; *Kay and Kay*, 1985], and of obducted arcs, which describe gabbros and diorites overlying both garnet granulites and mixtures of mafic and ultramafic cumulates [*Burns*, 1985; *DeBari and Coleman*, 1989; *Khan et al.*, 1989; *Pearcy et al.*, 1990; *DeBari and Sleep*, 1991; *Miller and Christensen*, 1994; *Kelemen et al.*, 2003a; Green et al., submitted manuscript, 2003].

[50] The relative proportions of middle and lower crust that are present (based on crustal layer thicknesses in our velocity model) are similar to or lower than those dictated by most inferences based on obducted arcs or by some fractionation models based on xenoliths. Studies of sections of obducted arcs such as Kohistan and Talkeetna are often used to calculate relative proportions of various crustal compositions and thus derive mass balances or estimates of primary magma composition [*Pearcy et al.*, 1990; *DeBari and Sleep*, 1991]. For example, *DeBari and Sleep* [1991] report 18% ultramafic cumulates, 16% garnet- and spinel-bearing gabbros, 34% gabbros to tonalities, and 32% volcanic rocks across a representative section of the Talkeetna obducted arc, near Tonsina, AK. Likewise, the relative proportions of lower crust in other obducted arcs are as small as or smaller than observed in Tonsina (e.g., Talkeetna, Kohistan) [*DeBari and Coleman*, 1989; *DeBari and Sleep*, 1991; *Miller and Christensen*, 1994; *Kelemen et al.*, 2003a; Green et al., submitted manuscript, 2003]. Because exposed arc sections are incomplete, it is likely that the observed relative thicknesses of each arc unit are not representative of the original arc structure [*Pearcy et al.*, 1990]. More specifically, dense lower-crustal, ultramafic-mafic cumulates are more likely to be removed during obduction, if not before, than other arc sections due to their high density [*Jull and Kelemen*, 2001; *Kelemen et al.*, 2003a]. Most studies agree that these arcs were originally of comparable thickness to the crust in our model of the Aleutians (>30 km) and that they originally included thick sections of mafic cumulates (at least ~20 km), even if the entirety of these mafic sections are not preserved today [*DeBari and Coleman*, 1989; *Kelemen et al.*, 2003a; Green et al., submitted manuscript, 2003].

[51] Predictions from fractionation models based on xenoliths from the middle and lower crust of the Aleutian islands suggest similar relative proportions of arc materials to those interpreted in the layers of our velocity model [*Conrad and Kay*, 1984; *Kay and Kay*, 1985; *DeBari et al.*, 1986]. *Kay and Kay* [1985] use both calc-alkaline and tholeiitic fractionation trends and the major element geochemistry of extrusive materials along the arc to calculate relative proportions of upper and lower crust generated by fractionation of a common basaltic parental magma. In this calculation, the upper crust of the Aleutian arc includes basalt, high-Al basalt, andesite-basalt and andesite (and plutonic equivalents), and the parental magma is inferred to be similar to a olivine tholeiite that has a distinctive trace element and isotope chemistry inherited from the subducted slab and sediments. Their calculations yield a lower crust, composed of plagioclase-bearing cumulates and possibly ultramafic cumulates, whose volume is 150% of the corresponding upper crust. They also predict a layer of ultramafic-mafic cumulates near the crust-mantle boundary whose volume is 50% of the upper crust. In this case, their upper crust corresponds to our most shallow crustal layer, and all of the cumulates in their calculations (including plagioclase-bearing, mafic, and ultramafic) correspond to our middle and lower crust. Their predicted ratio of 1:2 of upper crust to middle and lower crust in our model compares well to the ratio of 1:2.5 present in our model. More recent crystallization experiments show that up to 60% of mantle-derived magmas might crystallize pyroxenites at high pressure (1.2 GPa) when high concentrations of H_2O (>3%) are present [*Müntener et al.*, 2001].

9.7. High-Velocity Lower Crust in Arc Segment Center

[52] On the eastern section of line A2, notably high velocities are found in the lower and middle crust in the vicinity of Unmak and Unalaska Islands (Figure 8). This portion of the arc roughly corresponds to the middle of a segment in the overriding plate. These segments often correspond to features on the subducting plate (i.e., Amlia, Adak, and Rat Fracture Zones), though not always [*Geist et al.*, 1988; *Kay and Kay*, 1994]. Definitions of plate segmentation based on structural investigations [*Geist et al.*, 1988; *Ryan and Scholl*, 1993], earthquake distribution [*Nishenko and Jacob*, 1990; *Lu and Wyss*, 1996] and geochemistry [*Kay et al.*, 1982; *Kay and Kay*, 1994] consistently identify a block, called Four Mountains [*Kay et al.*, 1982], occupying the portion of line A2 where the highest velocities are observed. The western portion of line

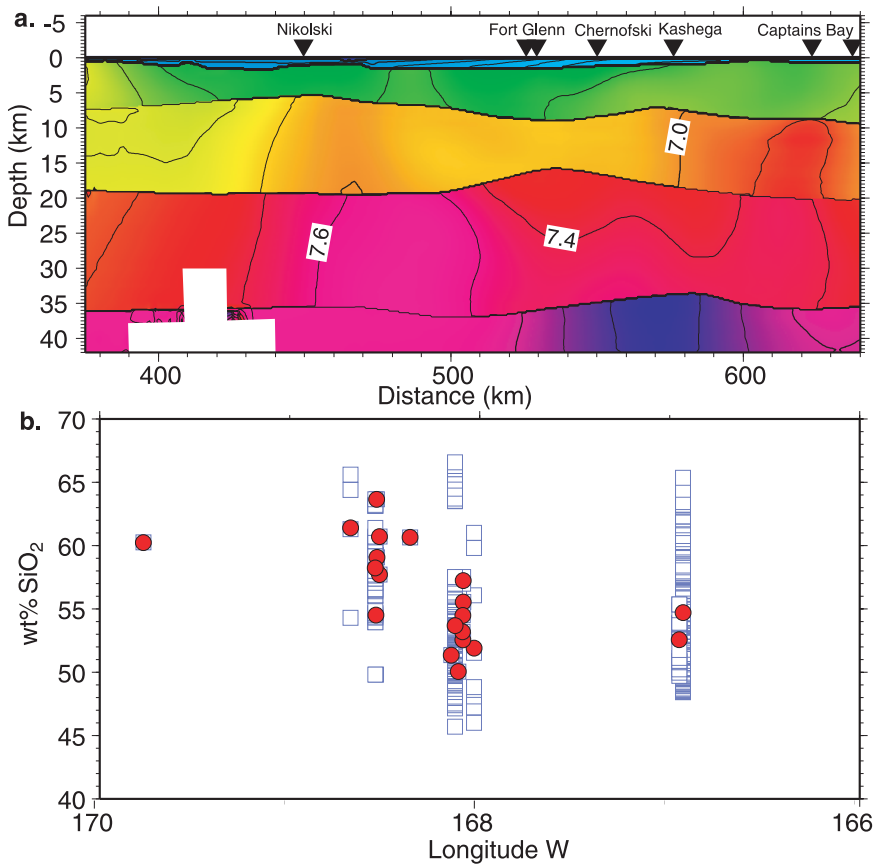

Figure 11. Velocity and weight percent SiO_2 in the central Aleutians around the Four Mountains block. (a) Velocity model around the Four Mountains block. Note the exceptionally high velocities in the lower crust that occur near the center of an arc segment (model km 475). (b) Weight percent SiO_2 around the Four Mountains block. Blue squares indicate the weight percent SiO_2 of each sample in the compilation, and red dots are average values of weight percent SiO_2 collected at the same location. These values are taken from the compilation of *Kelemen et al.* [2003c]. Note that high velocities in the lower crust appear to correspond to relatively high values of SiO_2 in lavas within this segment.

A2 lies in the Adreanof block, and the eastern portion resides in the Cold Bay block (Figures 1a and 10).

[53] The models of Kay and Kay imply that segment centers, where relatively little intra-arc extension is taking place, might host the production of comparatively felsic lavas by high-pressure fractionation of rising, mantle wedge derived magmas. Correspondingly, low-pressure fractionation, which would be expected to yield more mafic lavas, might occur at segment edges [*Kay et al.*, 1982; *Kay and Kay*, 1994]. If primary magma compositions are relatively constant, but extrusive volcanism is more felsic in segment centers, a larger volume of mafic residua of fractionation must reside in the lower or middle crust beneath these more felsic magmatic centers. One explanation for the high velocities observed in the lower crust around model km 475 is that it is composed of the mafic cumulates necessary to create the relatively felsic surface volcanics and shallow plutons.

[54] Further evidence for the correspondence of relatively felsic volcanism with more mafic residue is provided by the geochemistry of volcanoes on Umnak Island, which straddles the Cold Bay and Four Mountains blocks, as defined by *Kay et al.* [1982] (Figures 1 and 10). Okmok and Recheshnoi volcanoes are 50 km apart, yet have different major element compositions and corresponding fractionation trends [*Miller et al.*, 1992]; Okmok is relatively mafic and tholeiitic, while Recheshnoi is relatively felsic and calc-alkaline. In our velocity model, Recheshnoi and Okmok are at model km ~475 and 520, respectively (Figure 8). Note the change in lower-crustal velocities over this interval, from ~7.7 km/s beneath the more felsic Recheshnoi to 7.5 km/s beneath the more mafic

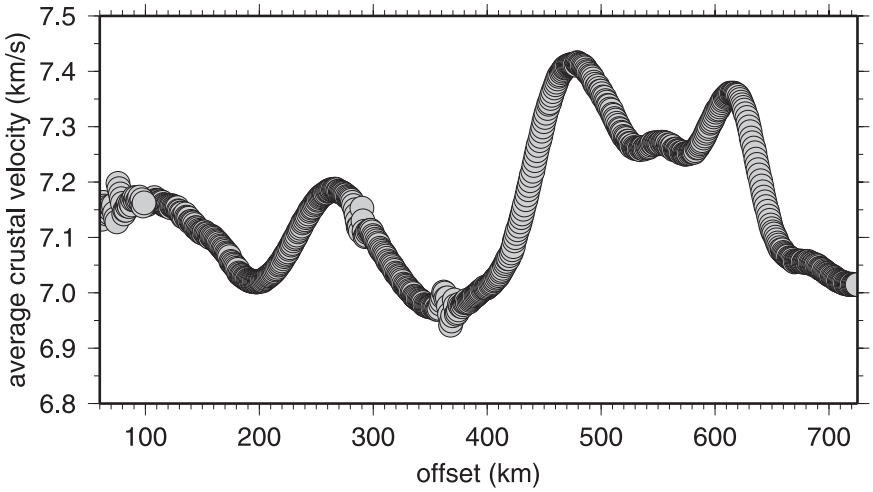

Figure 12. Average crustal P wave velocity for depths >10 km. Velocity values shallower than 10 km are excluded because these velocities are affected by variable porosity and fracture distribution [*Carlson and Gangi*, 1985]. Note that there is a westward decrease in average crustal velocity.

Okmok. Figure 11 shows a section of our velocity model around the Four Mountains block together with a plot of wt% SiO_2 for lavas in the same area, which demonstrates a first-order anticorrelation between lower-crustal velocity and SiO_2 content of lavas.

[55] Lateral variations in temperature also likely contribute to for velocity variation in the lower crust within arc segments. As mentioned before, the edges of structural blocks are probably associated with intra-arc extension. This extension may allow warm material to rise to shallower levels of the arc at arc segment edges than in arc segment centers [*Singer and Myers*, 1990; *Singer et al.*, 1992]. In this case, higher geothermal gradients and lower seismic velocities would be expected near segment edges and lower geothermal gradients and higher seismic velocities would be expected in segment centers. A variation of ~750°C, calculated using a dV/dT of 5.6×10^{-4} [*Korenaga et al.*, 2002], would be required to produce observed along-arc variations in velocity. As such extreme temperature variations are unlikely, we conclude that temperature changes contribute to, but are not solely responsible for, along-arc velocity variations.

[56] Higher temperatures and low-pressure fractionation associated with segment edges would be expected to produce lower velocities than the cooler temperatures and high-pressure fractionation associated with segment centers. Consequently, we assert that variable composition of mafic cumulates and, to a lesser extent, variable thermal gradients in the arc crust explain the high velocity lower crust within the arc segment (Figure 10).

9.8. Average Crustal Velocity and Major Element Composition

[57] Average crustal velocity is a useful parameter for evaluating crustal composition because it represents the bulk composition of arc material regardless of modifications that create variations in middle- or lower-crustal velocity [e.g., *Smithson et al.*, 1981; *Kelemen and Holbrook*, 1995]. Primitive lava compositions (Mg # > 0.6), which have undergone little crustal modification from possible primary magmas (Mg # > ~0.7), should also represent the composition of material added to the arc prior to crustal differentiation. Along line A2, average crustal velocities below 10 km increase eastward in the central Aleutians from 174° to 164° longitude (Figure 12). This first-order change in average crustal velocity roughly corresponds to trends in the composition of primitive lavas. On the scale of the entire oceanic Aleutian arc, from 165°E to 165°W, there are clear major element trends in which MgO increases and SiO_2 decreases eastward [*Kelemen et al.*, 2003c] (Figure 13). Even in the range of latitude covered by line A2, less obvious but similar trends are observed (Figure 13). While seismic data along line A2 are too coarse and geochemical trends too subtle to provide definitive evidence for a link between average crustal

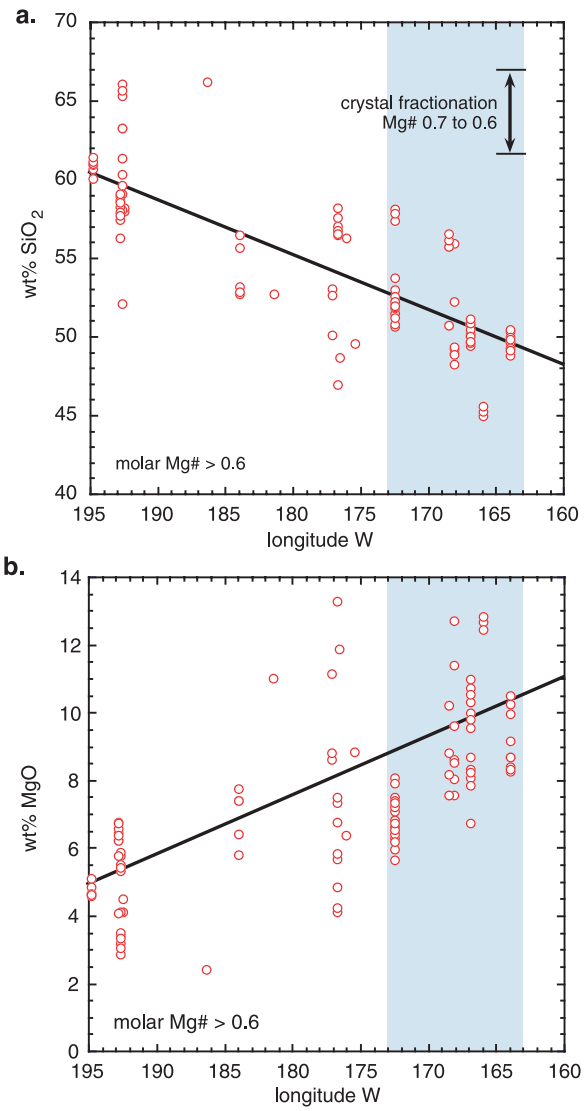

Figure 13. Major element geochemistry along the entire Aleutian arc taken from *Kelemen et al.* [2003c]. Red circles indicate data values. Linear trend lines were fit to each these data sets and are plotted as thin black lines. Note the westward increase in SiO_2 and decrease in MgO along the Aleutian arc. (a) Weight percent (wt %) SiO_2 for lavas with Mg # > 0.6; (b) wt % MgO for lavas with Mg # > 0.6. The blue bar indicates the range of longitudes spanned by line A2.

velocity and surface geochemistry, these data do imply a first-order correlation.

[58] Calculations using the relationship of SiO_2 and MgO to velocity given by *Kelemen and Holbrook* [1995] show that the magnitude of variation of crustal velocity across the central Aleutians (e.g., the change in velocity between model km 100–350 and 450–650) is consistent with variations in SiO_2 and MgO taken from the trend lines on Figures 13a and 13b. The relationship between wt% SiO_2 and wt% MgO and P wave velocity can be expressed as follows [*Kelemen and Holbrook*, 1995]:

$$V_p = 8.054 - 0.024 \text{ wt\% } SiO_2 + 0.029 \text{ wt\% MgO}$$

The values for wt% SiO_2 and wt% MgO at the western end of line A2 (taken from the linear trend line) are 53.25 and 7.5, and together these predict an average V_p of 6.99 km/s. Likewise, values for wt% SiO_2 and wt% MgO at the eastern end of line A2 are 49.1 and 9.7, and they predict an average V_p of 7.16 km/s. For observed changes in SiO_2 and MgO across the central Aleutians, a ~0.16 km/s change in average crustal velocity should be observed between the western and eastern ends of line A2. Absolute values of calculated V_p compare well to the values predicted above, though slightly higher, where 7.09 km/s is the average V_p at the western end of line A2 (model km 100–300) and 7.22 is the V_p at the eastern end (model km 400–650). Perhaps more important than the absolute correspondence of V_p, wt% SiO_2 and wt% MgO is that the change in V_p across line A2, ~0.14 km/s, is consistent with observed changes in primitive lava compositions. In summary, relative changes in MgO and SiO_2 predicted by primitive lavas are observed in average crustal velocity.

[59] If this correlation between primitive lavas and average crustal composition is significant, it suggests that major element geochemistry of lavas with Mg # > 0.6 is a good proxy for relative changes in average crustal compositions of arcs. While this correlation is tenuous in the central Aleutians, where major element trends in primitive lavas are weak, we anticipate a more robust correspondence between geochemistry and average velocity in island arcs where along-arc changes in subduction parameters (e.g., convergence rate and obliquity, age of subducting plate) are more dramatic.

[60] Along-arc changes in primitive lava composition and average crustal velocity along line A2 might be explained by a westward increase in subduction obliquity or a westward decrease in the age of the subducting plate [*Defant and Drummond*, 1990; *Yogodzinski et al.*, 1995; *Green and Harry*, 1999]. The same trends in major element composition are more pronounced further west, where subduction is considerably more oblique and subducting oceanic crust is

younger [*Yogodzinski et al.*, 1995; *Kelemen et al.*, 2003c].

9.9. Implications for the Creation of Continental Crust

[61] The bulk composition of the central Aleutian island arc, derived from seismic velocity, is significantly more mafic than average continental crust; the lower crust, particularly, creates challenges for models that require the accretion of island arcs to create continental crust, as it appears to be composed of ultramafic-mafic cumulates. However, there are some components of the arc that might contribute to the formation of continental crust. While the middle crust of the central Aleutians has a higher average velocity than continental crust at similar depths (6.31–6.47 km/s), it does resemble lower continental crust (6.78–7.02 km/s) [*Christensen and Mooney*, 1995]. As a result, it is possible that the upper and middle crust might be suitable building blocks for continental crust. However, the high-velocity lower crust in the Aleutian arc would need to be significantly modified in order to have velocities similar to continental lower-crustal velocities or might need to be removed altogether [*Kay and Kay*, 1988; *Kay and Kay*, 1993; *Jull and Kelemen*, 2001].

10. Conclusions

[62] A new velocity model along line A2, which parallels the central Aleutian island arc, indicates high velocities of 6.5–7.3 km/s in the middle crust and 7.3–7.7 km/s in lower crust and a total crustal thickness of 35–37 km. Our analysis uses a well-constrained 3-D ray tracing/2.5-D inversion technique to model this sparse, 3-D data set and incorporates information on shallow velocity structure to limit the propagation of shallow velocity structure deeper in the model. The resulting velocity model differs from previously published models generated from this data set in that it contains greater lateral continuity and vertical stratification, and consistently higher middle- and lower-crustal velocities. Middle-crustal velocities together with outcrop geology and recent calculations of velocity for igneous assemblages over a range of pressures and temperatures suggest that the middle crust is composed primarily of plutons with basaltic and andesitic compositions [*Kay et al.*, 1990; *Kelemen*, 1995; *Behn and Kelemen*, 2003; *Kelemen et al.*, 2003a]. High velocities in the lower crust suggest that it is composed of ultramafic-mafic cumulates and/or garnet granulites [*Miller and Christensen*, 1994; *Christensen and Mooney*, 1995; *Behn and Kelemen*, 2003]. The highest lower-crustal velocities along line A2 are located in the center of an arc segment and likely represent the mafic residua of high-pressure fractionation and lower temperatures in the comparatively compressive stress regime. Trends in the composition of primitive lavas (Mg # > 0.6) match along-arc variations in average crustal velocity to the first order, although trends in both composition and velocity data in this part of the Aleutian island arc are very subtle. Finally, although the Aleutian arc crust as a whole is significantly more mafic than average continental crust, the upper and middle crust might be suitable building blocks for continental crust if the lower crust were significantly modified or removed by delamination.

Acknowledgments

[63] We gratefully acknowledge Moritz Fliedner and Simon Klemperer, who provided digital versions of their velocity models and other valuable information on the Aleutians experiment, Sue McGeary, who provided MCS shot gathers from line A2, and Daniel Lizarralde, who provided data from ocean bottom seismometers on line A2 and useful discussions. Receiver gathers recorded by land seismometers were acquired from the IRIS Data Management Center. We would also like to thank Geoffrey Abers, John Hole, and Jim Gaherty for their thoughtful and thorough reviews, which greatly improved this manuscript. Funding for this work was provided by the University of Wyoming Graduate School.

References

Abers, G. A. (1994), Three-dimensional inversion of regional P and S arrival times in the East Aleutians and sources of subduction zone gravity highs, *J. Geophys. Res.*, *99*, 4395–4412.

Arndt, N. T., and S. L. Goldstein (1989), An open boundary between continental crust and mantle: Its role in crust formation and crustal recycling, *Tectonophysics*, *161*, 201–212.

Baker, D. R., and D. H. Eggler (1983), Fractionation paths of Atka (Aleutians) high-alumina basalts; constraints from phase relations, *J. Volcanol. Geotherm. Res.*, *18*(1–4), 387–404.

Behn, M. D., and P. B. Kelemen (2003), Relationship between seismic P-wave velocity and the composition of anhydrous igneous and meta-igneous rocks, *Geochem. Geophys. Geosyst.*, *4*(5), 1041, doi:10.1029/2002GC000393.

Ben-Avraham, Z., and A. K. Cooper (1981), Early evolution of the Bering Sea by collision of oceanic rises and North Pacific subduction zones, *Geol. Soc. Am. Bull.*, *92*, 485–495.

Braile, L. W., W. J. Hinze, R. R. B. von Frese, and G. R. Keller (1989), Seismic properties of the crust and uppermost mantle of the conterminous United States and adjacent Canada, in *Geophysical Framework of the Continental United States*, edited by L. C. Pakiser and W. D. Mooney, Geol. Soc. Am. Mem., 172, 655–680.

Brophy, J. G. (1989), Basalt convection and plagioclase retention; a model for the generation of high-alumina arc basalt, *J. Geol.*, *97*(3), 319–329.

Burns, L. E. (1985), The Border Range ultramafic and mafic complex, south-central Alaska: Cumulate fractionates of island-arc volcanics, *Can. J. Earth Sci.*, *22*, 1020–1038.

Carlson, R. L., and A. F. Gangi (1985), Effect of cracks on the pressure dependence of P wave velocities in crystalline rocks, *J. Geophys. Res.*, *90*, 8675–8684.

Christensen, N. I., and W. D. Mooney (1995), Seismic velocity structure and composition of the continental crust: A global view, *J. Geophys. Res.*, *100*, 9761–9788.

Class, C., D. M. Miller, S. L. Goldstein, and C. H. Langmuir (2000), Distinguishing melt and fluid subduction components in Umnak volcanics, Aleutian Arc, *Geochem. Geophys. Geosyst.*, *1*, doi:10.1029/1999GC000010.

Coats, R. R. (1952), Magmatic differentiation in Tertiary and Quaternary volcanic rocks from Adak and Kanaga Islands, Aleutian Islands, Alaska, *Geol. Soc. Am. Bull.*, *63*, 486–514.

Conrad, W. K., and R. W. Kay (1984), Ultramafic and mafic inclusions from Adak Island: Crystallization history, and implications for the nature of primary magmas and crustal evolution of the Aleutian Arc, *J. Petrol.*, *25*, 88–125.

Cooper, A. K., M. S. Marlow, D. W. Scholl, and A. J. Stevenson (1992), Evidence for Cenozoic extension in the Bering Sea Region, *Tectonics*, *11*(4), 719–731.

DeBari, S. M., and R. G. Coleman (1989), Examination of the deep levels of an island arc: Evidence from the Tonsina ultramafic-mafic assemblage, Tonsina, Alaska, *J. Geophys. Res.*, *94*, 4373–4391.

DeBari, S. M., and N. H. Sleep (1991), High-Mg, low-Al bulk composition of the Talkeetna island arc, Alaska: Implications for primary magmas and the nature of arc crust, *Geol. Soc. Am. Bull.*, *103*, 37–47.

DeBari, S., S. M. Kay, and R. W. Kay (1986), Ultramafic xenoliths from Adagdak Volcano, Adak, Aleutian Islands, Alaska: Deformed igneous cumulates from the Moho of an Island Arc, *J. Geol.*, *95*, 329–341.

Defant, M. J., and M. S. Drummond (1990), Derivation of some modern arc magmas by melting of young subducted lithosphere, *Nature*, *347*, 662–665.

DeMets, C., and T. H. Dixon (1999), New kinematic models for Pacific-North America motion from 3 Ma to present: I. Evidence for steady motion and biases in the NUVEL-1A model, *Geophys. Res. Lett.*, *26*(13), 1921–1924.

Ekström, G., and E. R. Engdahl (1989), Earthquake source parameters and stress distribution in the Adak Island region of the central Aleutian Islands, Alaska, *J. Geophys. Res.*, *94*, 15,499–15,519.

Engdahl, E. R., S. Billington, and C. Kisslinger (1989), Teleseismically recorded seismicity before and after the May 7, 1986, Andreanof Islands, Alaska, earthquake, *J. Geophys. Res.*, *94*, 15,481–15,498.

Fliedner, M. M., and S. L. Klemperer (1999), Structure of an island-arc: Wide-angle seismic studies in the eastern Aleutian Islands, Alaska, *J. Geophys. Res.*, *104*, 10,667–10,694.

Fliedner, M. M., and S. L. Klemperer (2000), Crustal structure transition from oceanic arc to continental arc, eastern Aleutian Islands and Alaska Peninsula, *Earth Planet. Sci. Lett.*, *179*, 567–579.

Fournelle, J. H., B. D. Marsh, and J. D. Myers (1994), Age, character, and significance of Aleutian arc volcanism, in *Geology of North America*, vol. G-1, *The Geology of Alaska*, edited by G. Plafker and H. C. Berg, pp. 723–757, Geol. Soc. of Am., Boulder, Colo.

Ganchin, Y. V., S. B. Smithson, I. B. Morozov, D. K. Smythe, V. Z. Garipov, N. A. Karaev, and Y. Kristofferson (1998), Seismic studies around the Kola Superdeep Borehole, Russia, *Tectonophysics*, *288*, 1–16.

Geist, E. L., J. R. Childs, and D. W. Scholl (1988), The origin of summit basins of the Aleutian Ridge: Implications for block rotation of an arc massif, *Tectonics*, *7*(2), 327–341.

Gladczenko, T. P., M. F. Coffin, and O. Eldholm (1997), Crustal structure of the Ontong Java Plateau: Modeling of new gravity and existing seismic data, *J. Geophys. Res.*, *102*, 22,711–22,729.

Green, N. L., and D. L. Harry (1999), On the relationship between subducted slab age and arc basalt petrogenesis, Cascadia subduction system, North America, *Earth Planet. Sci. Lett.*, *171*, 367–381.

Hamilton, W. B. (1988), Plate tectonics and island arcs, *Geol. Soc. Am. Bull.*, *100*, 1503–1527.

Hasegawa, A., D. Zhao, S. Hori, A. Yamamoto, and S. Horiuchi (1991), Deep structure of the northeastern Japan arc and its relationship to seismic and volcanic activity, *Nature*, *352*, 683–689.

Hirose, K. (1997), Melting experiments on lherzolite KLB-1 under hydrous conditions and generation of high-magnesian andesitic melts, *Geology*, *25*(1), 42–44.

Holbrook, W. S., D. Lizarralde, S. McGeary, N. Bangs, and J. Diebold (1999), Structure and composition of the Aleutian island arc and implication for continental crustal growth, *Geology*, *27*(1), 31–34.

Hole, J. A. (1992), Nonlinear high-resolution three-dimensional seismic travel time tomography, *J. Geophys. Res.*, *97*, 6553–6562.

Hole, J. A., and B. C. Zelt (1995), 3-D finite-difference reflection traveltimes, *Geophys. J. Int.*, *121*, 427–434.

Hyndman, R. D., and S. M. Peacock (2003), Serpentinization of the forearc mantle, *Earth Planet. Sci. Lett.*, *212*, 417–432.

Intergovernmental Oceanographic Commission and International Hydrographic Organization (2003), *GEBCO Digital Atlas* [CD-ROM], centenary ed., Br. Oceanogr. Data Cent., Liverpool, U. K.

Johnson, C. A., and E. I. Essene (1982), The formation of garnet in the olivine-bearing metagabbros from the Adirondacks, *Contrib. Mineral. Petrol.*, *81*, 240–251.

Jull, M., and P. B. Kelemen (2001), On the conditions for lower crustal convective instability, *J. Geophys. Res.*, *106*, 6423–6446.

Kay, R. W. (1978), Aleutian magnesian andesites; melts from subducted Pacific Ocean crust, *J. Volcanol. Geotherm. Res.*, *4*, 117–132.

Kay, R. W., and S. M. Kay (1988), Crustal recycling and the Aleutian arc, *Geochim. Cosmochim. Acta*, *52*, 1351–1359.

Kay, R. W., and S. M. Kay (1993), Delamination and delamination magmatism, *Tectonophysics*, *219*, 177–189.

Kay, S. M., and R. W. Kay (1985), Role of crystal cumulates and the oceanic crust in the formation of the lower crust of the Aleutian arc, *Geology*, *13*, 461–464.

Kay, S. M., and R. W. Kay (1994), Aleutian magmas in space and time, in *Geology of North America*, vol. G-1, *The Geology of Alaska*, edited by G. Plafker and H. C. Berg, pp. 687–722, Geol. Soc. of Am., Boulder, Colo.

Kay, S. M., R. W. Kay, and G. P. Citron (1982), Tectonic controls of tholeiitic and calc-alkaline magmatism in the Aleutian arc, *J. Geophys. Res.*, *87*, 4051–4072.

Kay, S. M., R. W. Kay, and M. R. Perfit (1990), Calc-alkaline plutonism in the intraoceanic Aleutian arc, Alaska, in *Plutonism From Antarctica to Alaska*, edited by S. M. Kay and C. W. Rapela, *Spec. Pap. Geol. Soc. Am.*, *241*, 233–255.

Kelemen, P. B. (1995), Genesis of high Mg# andesites and the continental crust, *Contrib. Mineral. Petrol.*, *120*, 1–19.

Kelemen, P. B., and W. S. Holbrook (1995), Origin of thick, high-velocity igneous crust along the U.S. East Coast Margin, *J. Geophys. Res.*, *100*, 10,077–10,094.

Kelemen, P. B., K. Hangøf, and A. R. Greene (2003a), One view of the geochemistry of subduction-related magmatic arcs, with an emphasis on primitive andesite and lower crust, in *The Crust*, pp. 593–659, edited by R. L. Rudnick, Elsevier Sci., New York.

Kelemen, P. B., J. L. Rilling, E. M. Parmentier, L. Mehl, and B. R. Hacker (2003b), Thermal structure due to solid-state flow in the mantle wedge beneath arcs, in *Inside the Subduction Factory*, *Geophys. Monogr. Ser.*, vol. 138, edited by J. Eiler, pp. 293–311, AGU, Washington, D. C.

Kelemen, P. B., G. M. Yogodzinski, and D. W. Scholl (2003c), Along-strike variation in the Aleutian Island Arc: Genesis of high Mg# andesite and implications for continental crust, in *Inside the Subduction Factory*, *Geophys. Monogr. Ser.*, vol. 138, edited by J. Eiler, pp. 223–276, AGU, Washington, D. C.

Khan, M. A., M. Q. Jan, B. F. Windley, J. Tarney, and M. F. Thirlwall (1989), The Chilas mafic-ultra-mafic igneous complex; the root of the Kohistan island arc in the Himalaya of northern Pakistan, in *Tectonics of the Western Himalayas*, edited by L. L. Malinconico, Jr. and R. J. Lillie, *Spec. Pap. Geol. Soc. Am.*, *232*, 75–94.

Korenaga, J., P. B. Kelemen, and W. S. Holbrook (2002), Methods for resolving the origin of large igneous provinces from crustal seismology, *J. Geophys. Res.*, *107*(B9), 2178, doi:10.1029/2001JB001030.

Krol, M. A., P. K. Zeitler, and P. Copeland (1996), Episodic unroofing of the Kohistan Batholith, Pakistan: Implications from K-felspar thermochronology, *J. Geophys. Res.*, *101*, 28,149–28,164.

Lizarralde, D., W. S. Holbrook, S. McGeary, N. Bangs, and J. Diebold (2002), Crustal construction of a volcanic arc, wide-angle seismic results from the western Alaska Peninsula, *J. Geophys. Res.*, *107*(8), 2164, doi:10.1029/2001JB000230.

Lonsdale, P. (1988), Paleogene history of the Kula plate: Offshore evidence and onshore implications, *Geol. Soc. Am. Bull.*, *10*(5), 733–754.

Lu, Z., and M. Wyss (1996), Segmentation of the Aleutian plate boundary derived from stress direction estimates based on fault plane solutions, *J. Geophys. Res.*, *101*, 803–816.

Mann, D., and J. Freymuller (2003), Volcanic and tectonic deformation on Unimak Island in the Aleutian arc, Alaska, *J. Geophys. Res.*, *108*(B2), 2108, doi:10.1029/2002JB001925.

Mann, D., J. Freymuller, and Z. Lu (2002), Deformation associated with the 1997 eruption of Okmok volcano, Alaska, *J. Geophys. Res.*, *107*(B4), 2072, doi:10.1029/2001JB000163.

Marlow, M. S., and A. K. Cooper (1983), Wandering terranes in southern Alaska: The Aleutia Microplate and implications for the Bering Sea, *J. Geophys. Res.*, *88*, 3439–3446.

Marsh, B. D., and I. S. E. Carmichael (1974), Benioff zone magmatism, *J. Geophys. Res.*, *79*, 1196–1206.

McBirney, A. R., H. P. Taylor, and R. L. Armstrong (1987), Paricutin re-examined: A classic example of crustal assimilation in calc-alkaline magma, *Contrib. Mineral. Petrol.*, *95*, 4–20.

McCaffrey, R. (1996), Estimates of modern arc-parallel strain rates in fore arcs, *Geology*, *24*(1), 27–30.

McGeary, S., and A. W. Group (1996), Deep seismic profiling of the Aleutian arc and Bering Shelf, *Eos. Trans. AGU*, *77*(46), Fall Meet. Suppl., F659.

McLennan, S. M., and S. R. Taylor (1982), Geochemical constraints on the growth of the continental crust, *J. Geol.*, *90*, 347–361.

Miller, D. J., and N. I. Christensen (1994), Seismic signature and geochemistry of an island arc: A multidisciplinary study of the Kohistan accreted terrane, northern Pakistan, *J. Geophys. Res.*, *99*, 11,623–11,642.

Miller, D. M., C. H. Langmuir, S. L. Goldstein, and A. L. Franks (1992), The importance of parental magma composition to the calc-alkaline and tholeiitic evolution: Evidence from Umnak Island in the Aleutians, *J. Geophys. Res.*, *97*, 321–343.

Müntener, O., P. B. Kelemen, and T. L. Grove (2001), The role of H_2O during crystallization of primitive arc magmas under uppermost mantle conditions and genesis of igneous pyroxenites: An experimental study, *Contrib. Mineral. Petrol.*, *141*, 643–658.

Myers, J. D. (1988), Possible petrogenetic relations between low- and high-MgO Aleutian basalts, *Geol. Soc. Am. Bull.*, *100*, 1040–1053.

Myers, J. D., and T. J. McElfresh (2001), A relational database schema for managing geochemical and visual data; the Aleutian Arc Data System (AADS), *Geol. Soc. Am. Abstr. Programs*, *33*(6), 336.

Myers, J. D., B. D. Marsh, and A. K. Sinha (1985), Strontium isotopic and selected trace element variations between two Aleutian volcanic centers (Adak and Atka): Implications for the development of arc volcanic plumbing systems, *Contrib. Mineral. Petrol.*, *91*, 221–234.

Nishenko, S. P., and K. H. Jacob (1990), Seismic potential of the Queen Charlotte-Alaska-Aleutian seismic zone, *J. Geophys. Res.*, *95*, 2511–2532.

Pearcy, L. G., S. M. DeBari, and N. H. Sleep (1990), Mass balance calculations for two sections of island arc crust and implications for formation of continents, *Earth Planet. Sci. Lett.*, *96*, 427–442.

Plafker, G., J. C. Moore, and G. R. Winkler (1994), Geology of the southern Alaska margin, in *Geology of North America*, vol. G-1, *The Geology of Alaska*, edited by G. Plafker and H. C. Berg, pp. 389–449, Geol. Soc. of Am., Boulder, Colo.

Plank, T., and C. H. Langmuir (1988), An evaluation of the global variations in the major element chemistry of arc basalts, *Earth Planet. Sci. Lett.*, *90*, 349–370.

Rudnick, R. L. (1995), Making continental crust, *Nature*, *378*, 571–578.

Rudnick, R. L., and D. M. Fountain (1995), Nature and composition of the continental crust: A lower crustal perspective, *Rev. Geophys.*, *33*(3), 267–309.

Ryan, H. F., and D. W. Scholl (1993), Geologic implications of great interplate earthquakes along the Aleutian Arc, *J. Geophys. Res.*, *98*, 22,135–22,146.

Singer, B. S., and J. D. Myers (1990), Intra-arc extension and magmatic evolution in the central Aleutian arc, Alaska, *Geology*, *18*, 1050–1053.

Singer, B. S., J. D. Myers, and C. D. Frost (1992), Mid-Pleistocene basalt from the Seguam Volcanic Center, central Aleutian Arc, Alaska: Local lithospheric structures and source variability in the Aleutian Arc, *J. Geophys. Res.*, *97*, 4561–4578.

Smithson, S. B., R. A. Johnson, and Y. K. Wong (1981), Mean crustal velocity: A critical parameter for interpreting crustal

structure and crustal growth, *Earth Planet. Sci. Lett.*, *53*, 323–332.

Suyehiro, K., N. Takahashi, Y. Ariie, Y. Yokoi, R. Hino, M. Shinohara, T. Kanazawa, N. Hirata, H. Tokuyama, and A. Taira (1996), Continental crust, crustal underplating, and low-Q upper mantle beneath an oceanic island arc, *Science*, *272*, 390–392.

Tatsumi, Y. (2001), Geochemical modeling of partial melting of subducting sediments and subsequent melt-mantle interaction: Generation of high-Mg andesites in the Setouchi volcanic belt, southwest Japan, *Geology*, *29*(4), 323–326.

Taylor, S. R. (1967), The origin and growth of continents, *Tectonophysics*, *4*(1), 17–34.

Vallier, T. L., D. W. Scholl, M. A. Fisher, T. R. Bruns, F. H. Wilson, R. von Huene, and A. J. Stevenson (1994), Geologic framework of the Aleutian arc, Alaska, in *Geology of North America*, vol. G-1, *The Geology of Alaska*, edited by G. Plafker, and H. C. Berg, pp. 367–388, Geol. Soc. of Am., Boulder, Colo.

Van Avendonk, H. J. A., A. J. Harding, J. A. Orcutt, and J. S. McClain (2001), Contrast in crustal structure across the Clipperton transform fault from travel time tomography, *J. Geophys. Res.*, *106*, 10,961–10,981.

Van Avendonk, H. J. A., D. J. Shillington, W. S. Holbrook, and M. J. Hornbach (2004), Inferring crustal structure in the Aleutian island arc from a sparse wide-angle seismic data set, *Geochem. Geophys. Geosyst.*, *5*, Q08008, doi:10.1029/2003GC000664.

Yogodzinski, G. M., and P. B. Kelemen (1998), Slab melting in the Aleutians; implications of an ion probe study of clinopyroxene in primitive adakite and basalt, *Earth Planet. Sci. Lett.*, *158*, 53–65.

Yogodzinski, G. M., R. W. Kay, O. N. Volynets, A. V. Koloskov, and S. M. Kay (1995), Magnesian andesite in the western Aleutian Komandorsky region: Implications for slab melting and processes in the mantle wedge, *Geol. Soc. Am. Bull.*, *107*(5), 505–519.

Zelt, C. A., and R. B. Smith (1992), Seismic traveltime inversion for 2-D crustal velocity structure, *Geophys. J. Int.*, *108*, 16–34.

Zelt, C. A., and B. C. Zelt (1998), Study of out-of-plane effects in the inversion of refraction/wide-angle reflection traveltimes, *Tectonophysics*, *286*, 209–221.

Zhao, D., and A. Hasegawa (1994), Teleseismic evidence for lateral heterogeneities in the northwestern Japan arc, *Tectonophysics*, *237*, 189–199.